# Hydrogen Bus Technology Validation Program

**Andy Burke, Zach McCaffrey, Marshall Miller**
**Institute of Transportation Studies, UC Davis**

**Kirk Collier, Neal Mulligan**
**Collier Technologies, Inc.**

**Technology Provider: Collier Technologies, Inc.**

**Grant number: ICAT 01-7**
**Grantee: University of California, Davis**
**Date: May 12, 2005**

Conducted under a grant by the California Air Resources
Board of the California Environmental Protection Agency

The statements and conclusions in this Report are those of the grantee and not necessarily those of the California Air Resources Board. The mention of commercial products, their source, or their use in connection with material reported herein is not to be construed as actual or implied endorsement of such products

## Acknowledgments

Work on this program was funded by the Federal Transit Administration, the California Air Resources Board, and the Yolo-Solano Air Quality Management District.

This Report was submitted under Innovative Clean Air Technologies grant number 01-7 from the California Air Resources Board.

# Table of Contents

**Abstract…….....6**

**Executive Summary…….....7**

**1. Introduction……9**

**2. Emissions Standards……..9**

**3. Innovative Technology……..9**

**4. ICAT Project……..……...10**

**4.1 Engine Modifications……10**

**4.2 Engine Testing and Performance Maps…….....12**

**4.3 HCNG Combustion Modeling……..20**

**4.4 Transit Bus Simulations……21**

**4.5 Commercialization Costs…….....23**

**5. Status of Technology……26**

**6. Updated Commercialization Plan……..27**

**Appendix A. ……28**

# List of Figures

**Figure 1. Phase II modified HCNG engine on the Collier Technologies dynamometer ..….13**

**Figure 2. CNG Brake Thermal Efficiency (LHV)…….14**

**Figure 3. HCNG Brake Thermal Efficiency (LHV).....14**

**Figure 4. CNG Brake Specific $NO_X$ (g/bhph)…….…….....15**

**Figure 5. HCNG Brake Specific $NO_X$ (g/bhph)…….16**

**Figure 6. The HCNG bus……20**

**Figure 7. Speed versus time for the NYCCOMP drive cycle……...22**

**Figure 8. Speed versus time for the CBD14 drive cycle……...22**

**Figure 9. Speed versus time for the New York Bus drive cycle……...23**

# List of Tables

**Table 1. CARB Emissions Standards (g/bhp-hr) for Heavy-duty Engines……..9**

**Table 2. Results from Phase II engine dynamometer testing……...17**

**Table 3. Acceleration testing of the CNG and HCNG buses……18**

**Table 4. Emissions and fuel economy for the Daewoo 11.0 liter HCNG engine……19**

**Table 5. Results from Advisor simulations of CNG and HCNG buses……...24**

**Table 6. Estimated costs for hydrogen infrastructure for fleets of HCNG buses……..26**

## Abstract

Heavy duty engines are substantial contributors to $NO_X$ and PM emissions inventories in urban areas, and stringent emissions standards have been adopted as a consequence. CARB has passed very strict emissions standards for heavy duty engines beginning in 2007. Meeting these standards, especially for $NO_X$ emissions, may be difficult for conventional transit bus technologies. The purpose of the Hydrogen Bus Technology Evaluation Program was to develop and evaluate hydrogen enriched natural gas (HCNG) engine technology in transit buses and to demonstrate $NO_X$ emissions reductions below the CARB 2007 standards. Collier Technologies, Inc. modified a John Deere 8.1 liter natural gas engine to operate on a mixture of 30% hydrogen and 70% natural gas. The engine was tested on a dynamometer to determine emissions and fuel economy, and these values were compared with data from conventional CNG engines. UC Davis developed both an HCNG combustion model to understand the processes inside the engine and a dynamic vehicle model to understand the benefits of HCNG buses. The results indicate that HCNG bus $NO_X$ emissions can meet the CARB 2007 standards. Based on information from this program, Collier Technologies has developed a prototype HCNG engine which can be used to retrofit CNG buses.

## Executive Summary

The California Air Resources Board has approved very strict heavy duty emissions standards for transit bus engines. The CARB 2003 heavy duty emissions standard for $NO_X$ was 4 g/bhph. The standard for 2007 will be 0.2 g/bhph – a 95% reduction. Both commercial transit bus engine technologies, diesel and CNG, require significant after treatment technology to have a chance of meeting the 2007 standard.

The focus of the Hydrogen Bus Technology Validation Program ICAT project was to demonstrate that hydrogen enriched natural gas (HCNG) engines could meet this strict CARB standard.

Before the ICAT program began, Collier Technologies, Inc. modified a John Deere 8.1 liter engine to operate on HCNG fuel. This Phase I bus showed significant emissions reductions at modest powers but was unable to meet the 2007 standard. At high power, $NO_X$ emissions were well over 1.0 g/bhph. As part of the ICAT program, Collier Technologies made further modifications to the John Deere 8.1 liter engine. These Phase II modifications involved changes to the engine control program and replacing the stock turbocharger.

The Phase II engine was tested on a dynamometer to measure both emissions and fuel economy. The testing indicated significant tradeoffs between emissions and power. If the control strategy attempted to minimize emissions, the peak power of the engine was reduced. If power was not sacrificed, the emissions data at high torque exceeded the CARB 2007 standard for $NO_X$ by roughly a factor of 2. When the engine control is set to minimize emissions, the $NO_X$ emissions were below 0.2 g/bhph (the 2007 standard) for all measured torque-speed points.

Collier Technologies, Inc. used the information gained from the Phase II engine results to develop a commercial prototype HCNG engine. They choose to modify a Daewoo 11.0 liter CNG engine for HCNG operation. The larger engine allows them to de-rate the power while still having enough for transit bus purposes. Using this engine allows them to meet the 0.2 g/bhph $NO_X$ standard and still provide adequate power. Their commercialization plan now consists of marketing the modified Daewoo 11.0 liter engine to transit agencies as a replacement for the stock engine or to bus manufacturers as the stock engine.

The ICAT program involved several other tasks in addition to the design and testing HCNG engine. UC Davis researchers developed a combustion model to understand the characteristics of hydrogen enriched natural gas combustion, a dynamic vehicle model to estimate the benefits of HCNG buses, and cost models to estimate the cost to transit agencies of owning and operating HCNG buses.

An engine model with detailed chemical reactions was developed to predict the “in cylinder” production to $NO_X$ under realistic engine conditions. The model was able to predict measured $NO_X$ values over a large range of equivalence ratios. In particular, the results indicated that there is high sensitivity of $NO_X$ to equivalence ratio. For example, the variation in $NO_X$ between equivalence ratios of 0.7 and 0.6 can vary by almost an order of magnitude. Collier Technologies runs their engine at equivalence ratios below 0.6 in order to minimize $NO_X$.

The dynamic vehicle model was built on the Advisor vehicle platform. The bus was modeled using input files that simulated the Unitrans bus. CNG and HCNG engine maps for emissions and fuel economy were constructed from Collier technologies dynamometer data. Standard bus driving cycles, such as the Central Business District (CDB14) and the New York Bus (NYB), were used to estimate bus performance. As expected, $NO_X$ emissions were

significantly less for the HCNG bus compared to CNG buses. For the CBD14 drive cycle, HCNG bus $NO_X$ emissions were 6.6 grams/mile compared to 70.1 grams/mile for CNG buses. The fuel economy was 3.2 miles/gallon of diesel equivalent (2.7 miles/gallon of gasoline equivalent) for HCNG buses compared to 2.7 miles/gallon of diesel equivalent (2.3 miles/gallon of gasoline equivalent) for CNG buses.

A hydrogen fueling station cost model was used to estimate the cost to install and operate the hydrogen portion of a HCNG fueling station. It was assumed that transit agencies that adopted HCNG technology buses would already have CNG infrastructure in place. The cost model includes capital costs for hardware, installation costs, and operating costs including fuel (for example, natural gas for stations with reformers). Costs are near to midterm costs (0-5 years roughly). The costs were broken down into hardware, installation, contingency, energy, and fixed operating costs. The overall cost was estimated both as an annual cost over the lifetime of the station and as the cost for a kilogram of hydrogen dispensed (The energy in a kilogram of hydrogen is roughly equal to the energy of 0.88 gallons of diesel or 1.04 gallons of gasoline). For relatively small stations (100 kg/day) the cost of dispensed hydrogen was estimated at $15.04/gallon of diesel equivalent ($13.30/kg hydrogen). For larger stations (1000 kg/day) the cost for dispensed hydrogen was $7.38/gallon of diesel equivalent ($6.53/kg hydrogen).

## 1. Introduction

The Hydrogen Bus Technology Validation Program is a collaboration of private and public partners working together to evaluate hydrogen enriched natural gas (HCNG) bus technology. The intent of the program is to develop and test HCNG engines for transit buses in an effort to meet the strict CARB 2007 heavy duty emission standards. This report is the final element of an ICAT grant to develop HCNG technology.

## 2. Emissions Standards

Emission standards for engines have become increasingly stringent since 1985. The current standards in place for model year 2007 are quite demanding. Table 1 shows the standards for the various criteria pollutants. These standards are the basic requirements, but there are variations and exceptions given in detail in the regulations. In addition, there are optional standards that can be met under certain conditions. Engines must be tested and certified to these standards; otherwise, they cannot be used in transit buses.

**Table 1:CARB Emissions Standards (g/bhp-hr) for Heavy-duty Engines**

| Year | HC | CO | $NO_X$ | PM | Formaldehyde |
|---|---|---|---|---|---|
| 1985-1986 | 1.3 | 15.5 | 5.1 | NA | NA |
| 1988-1990 | 1.3 | 15.5 | 6 | 0.6 | NA |
| 1991-1993 | 1.3 | 15.5 | 5 | 0.1 | NA |
| 1994-1995 | 1.3 | 15.5 | 5 | 0.07 | NA |
| 1996-2003 | 1.3 | 15.5 | 4 | 0.05 | NA |
| 2004-2006[1] | 2.4 (plus $NO_X$) | 15.5 | 2.4 (plus NMHC) | 0.05 | NA |
| 2004-2006[2] (Diesel) | 0.5 | 5.0 | 0.5 | 0.01 | 0.01 |
| 2007 | 0.05 | 5.0 | 0.2 | 0.01 | 0.01 |

[1] Standards for $NO_X$ and hydrocarbons in the years 2004-2006 are given as the sum of the two pollutants (g/bhp-hr $NO_X$ + g/bhp-hr HC). Manufacturers can certify to 2.5 g/bhp-hr if the HC emissions are below 0.5 g/bhp-hr.

[2] Manufacturers can meet $NO_X$ and PM standards with base engine certified to the row above equipped with an aftertreatment system.

## 2. Innovative Technology

For heavy-duty applications using natural gas fuel, the technology that has been historically employed is to use lean burn as the mechanism to reduce $NO_X$ emissions. The limit on the ultimate $NO_X$ reduction capable by this technique is the point where the fuel does not burn completely with the amount of excess air required. This point is called the “lean limit” of combustion. The technology employed in this project is the use of hydrogen mixed with natural gas to create a fuel with much greater lean burn capability than natural gas alone. By extending the lean burn limit of the fuel, $NO_X$ emissions can be dramatically reduced when compared to natural gas alone.

The negative effect of using lean burn is that engine output power is reduced as less fuel is introduced for each unit of air processed by the engine. In addition, methods used by OEMs to extend the lean limit for natural gas, reduces the amount of air that can be effectively processed by the engine.

For this ICAT project, Collier Technologies modified a John Deere 8.1 liter natural gas transit bus engine to operate on the blend of hydrogen and natural gas. The engine modifications included enhanced air flow by replacing the stock turbocharger and changes to the engine timing using a modified engine controller. Initial work on the John Deere engine before this ICAT program (Phase I) resulted in improved emissions but significantly lowered power output.

The results of our project have demonstrated the efficacy of further extending the lean burn limit as a method to reduce $NO_X$ emissions over the current state of the art. It has further demonstrated that air flow to the engine must be enhanced if engine output power is to be maintained relative to the base engine operating on natural gas alone. The ICAT work (Phase II) resulted in an engine that meets the CARB standards for $NO_X$ and has improved power relative to the Phase I engine. The power is still somewhat reduced from the stock CNG engine.

The work on the Phase II portion of the bus program allowed Collier Technologies to develop a commercialization plan based on a Phase III engine. Phase III will focus on achieving technology that is suitable for implementation in transit buses throughout the United States. The goal is to achieve hardware that can be designated as U.S. manufacture through selective outsourcing of the components specifically designed for U.S. heavy duty vehicle integration with the HCNG fuel. To address the major issue of reduced power output due to ultra-lean burn conditions, Collier Technologies will base this new engine platform on an Daewoo 11L natural gas engine. The final product will be the demonstration of a dedicated HCNG heavy duty engine that can meet California's proposed 2007 emissions standards with no compromises to vehicle performance.

## 3. ICAT Program

The purpose of the Hydrogen Bus Technology Evaluation Program was to develop and evaluate hydrogen enriched natural gas (HCNG) engine technology in transit buses and to demonstrate $NO_X$ emissions reductions below the CARB 2007 standards. The project plan was to use information from the Phase I HCNG engine to design and produce a Phase II HCNG engine for testing. The specific goal was to produce an HCNG engine that was capable of meeting the CARB 2007 emissions standards for $NO_X$ (0.2 g/bhph) without sacrificing other engine capabilities such as power.

Section 3.1 will discuss Collier Technologies work in designing and modifying the John Deere 8.1 liter CNG engine for operation on HCNG fuel. Section 3.2 will discuss the testing of that modified engine. Sections 3.3 through 3.5 will describe the other ICAT tasks for this program. Those tasks include modeling of the combustion process, modeling of the HCNG bus, and estimating the commercialization costs for HCNG buses.

### 3.1 Engine modifications

Adding quantities of hydrogen to natural gas requires that significant amounts of charge dilution be employed so that $NO_X$ emissions are reduced. The charge dilution mechanism chosen for this conversion is lean burn. The measurement of the amount of lean burn is defined

by the term equivalence ratio. This is either defined as the ratio of the actual air-fuel ratio divided by the chemically correct air-fuel ratio called lambda, or the inverse of this ratio, called phi. Whichever term used, the amount of excess air entering the combustion chamber must be increased significantly to keep peak combustion temperatures low, thereby reducing the creation of oxides of nitrogen. The result of increasing the amount of air that does not participate in the combustion process is that engine power is dramatically reduced.

In order to make equivalent engine power with HCNG, the amount of air processed by the engine must increase. This project required the use of an existing 8.1L John Deere natural gas engine; therefore, increasing engine displacement to increase air flow was not reasonable. Also, this engine is already turbocharged which means that the only way to increase air flow is to increase turbocharger boost pressure.

In Phase I, the John Deere 8.1L engine was modified as follows:

1. The original Woodward electronic engine controller was replaced with a Motec system.
2. The original Bosch fuel injectors were replaced with Servojet injectors manufactured by Clean Air Power in San Diego, CA.
3. The original Air Research turbocharger was replaced with a custom-designed unit from Turbonetics.

The Woodward electronic controller that was originally used on the John Deere engine was replaced because control of the software was proprietary. It was replaced with a Motec unit to allow reprogramming of the fuel, ignition, and turbocharger control variables. The Motec unit was designed for the racing aftermarket and lacked much of the sophistication of the Woodward unit. The fuel injectors were replaced because the Motec could not control a number of injectors that were not an even multiple of the number of cylinders. The Servojet injectors individually flow more fuel than the Bosch injectors, but lack precise controllability when the fuel flow through the injectors is on for a short time interval. This lack of controllability caused higher than expected $NO_X$ emissions at idle.

The mechanism for achieving the low exhaust emissions from HCNG is to extend the lean limit of combustion. By doing this, less fuel is introduced into the engine for the same amount of air flow. If equivalent engine output power is to be achieved, more air must be introduced into each engine cylinder. The only way to accomplish this is to increase the turbocharger compressor outlet pressure. This creates two problems. One is that the air temperature increases with increasing pressure. The other is that the exhaust back pressure from the turbine section is increased as well. Again, as with the Motec engine controller, the source of hardware to accomplish higher boost pressures was the racing aftermarket. Although the boost pressure was successfully increased, the hardware used to accomplish this was not optimal. The inefficiencies exacerbated the two problems described earlier.

Although the emissions results from Phase I of the project were much lower than the OEM natural gas engine, they were not as low as the technology was capable of achieving. However, the experience gained from this project phase allowed us to make significant advances in Phase II of the project.

The most important change in preparing the Phase II engine was to return to the Woodward engine controller hardware. Access to the control software was obtained from Daewoo Heavy Industries. This controller is more sophisticated in its approach to fuel control for emissions. However, the control inputs to the Daewoo version of the controller are different

than the John Deere inputs. Therefore, the control inputs to the Woodward controller were modified to make the John Deere engine appear to be a Daewoo engine to the Woodward controller. This was accomplished by fabricating a custom toothed wheel that mounts to the camshaft of the John Deere engine. This tooth arrangement matched that of a Daewoo engine.

It was not possible to use the John Deere Woodward controller itself. Although the control algorithms for the John Deere and Daewoo controllers are identical, the software key was for the Daewoo controller only. Therefore, the wiring harness for the electronic engine controller had to be modified so that the proper pin locations were maintained between the John Deere engine and the Daewoo engine controller.

By using the Woodward controller, the John Deere Bosch fuel injector set up was maintained. This, along with the advanced control of the wide band oxygen sensor, improved the emissions performance dramatically from that achieved with the Phase I engine modifications.

The next major improvement in the Phase II engine was the modification of the existing John Deere turbocharger rather than using a racing aftermarket unit. Turbo Power in Placerville, CA was contacted to modify the existing John Deere turbocharger to increase boost pressure much more efficiently than with the Turbonetics turbocharger. An added benefit to this strategy was the incorporation of an integrated boost control valve. In Phase I, an external boost control valve was required which complicated the plumbing and control considerably.

Dynamometer testing was conducted that optimized fuel, spark timing, and boost control through the Woodward controller obtained from Daewoo. Emissions results were far superior to those obtained in Phase I of the project. Although, the maximum torque of the modified engine were about 20% lower than that achieved with the OEM natural gas engine, maximum engine horsepower was maintained. The equivalence ratio varied from 0.56-0.6 for the Phase II engine.

To help alleviate the lower peak torque situation, the control algorithms were modified to increase peak torque in the HCNG configuration by increasing fuel flow in certain critical areas of the fuel map. This strategy dramatically increases $NO_X$ emissions, but only in those driving situations where peak engine torque is required. An alternative to this strategy is to either change the gear ratio in the driveline differential and/or alter the shift algorithms in the automatic transmission.

### 3.2 Engine testing and performance maps

Both the modified Phase I and unmodified John Deere 8.1L natural gas engines were tested at Collier Technologies on an engine dynamometer. Each configuration was tested at various torque and speed points creating an engine map for both $NO_X$ emissions and fuel consumption (efficiency). The engine speed was varied from 800 – 2200 rpm. The unmodified engine torque varied between 25 and 750 ft-lbs. The modified engine torque varied between 25 and 644 ft-lbs. The peak power for the unmodified engine is 250 hp compared to a peak power for the modified engine of 212 hp. Figure 1 shows a picture of the modified engine connected to the dynamometer at Collier technologies.

The most important parameters for this project were engine output power, fuel efficiency, and $NO_X$ emissions. Collier Technologies did not have the capability to measure PM emissions on their dynamometer setup. Adding hydrogen to natural gas is expected to have little effect on PM emissions from the engine. We were not able to fully match the OEM power outputs for various reasons. First of all, in order to meet the maximum torque values published for this

engine, the air fuel ratio could not be made lean enough for low $NO_X$. Secondly, use of very high turbocharger boost pressures caused excessive air charge temperature for the intercooler on the bus. We compromised between $NO_X$ emissions under full power conditions, air charge temperature, and reduced engine output power. Figures 2 and 3 show the engine brake thermal efficiency as a function of engine torque and rpm for the OEM CNG configuration and the converted HCNG configuration respectively.

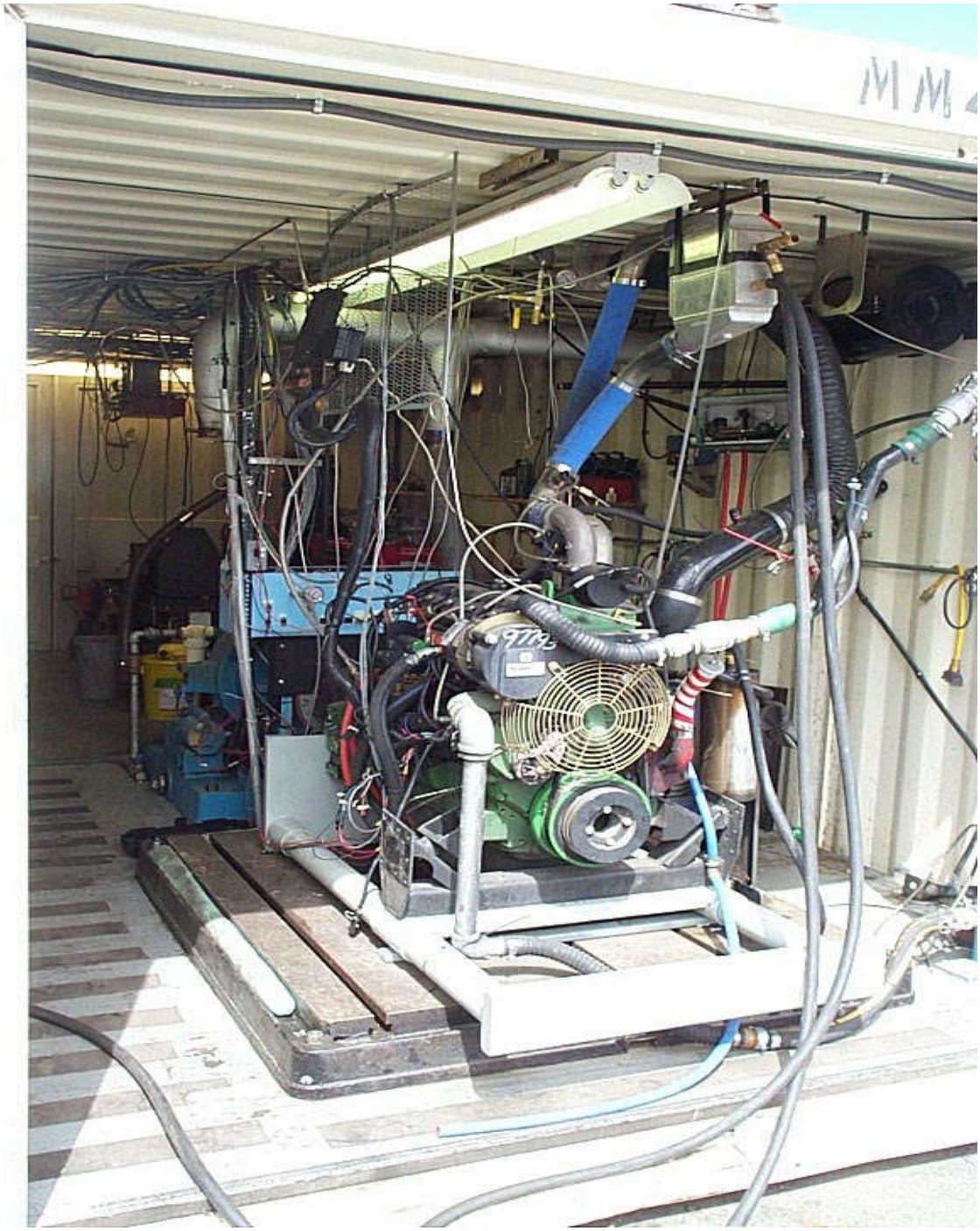

Figure 1. The Phase II modified HCNG engine on the Collier Technologies dynamometer.

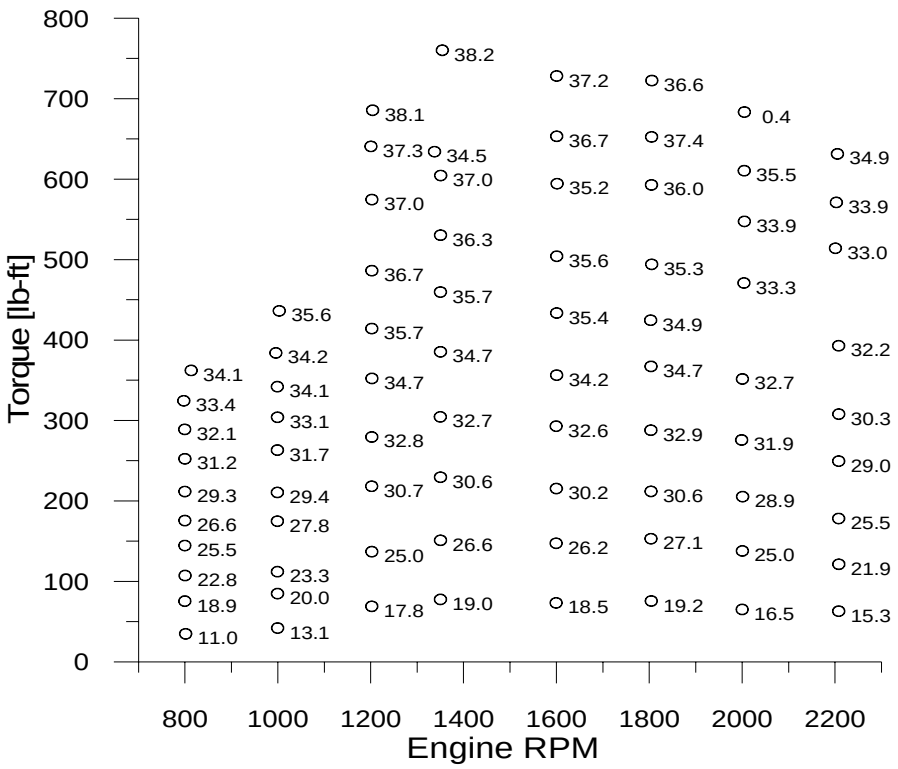


Figure 2. CNG Brake Thermal Efficiency (LHV)

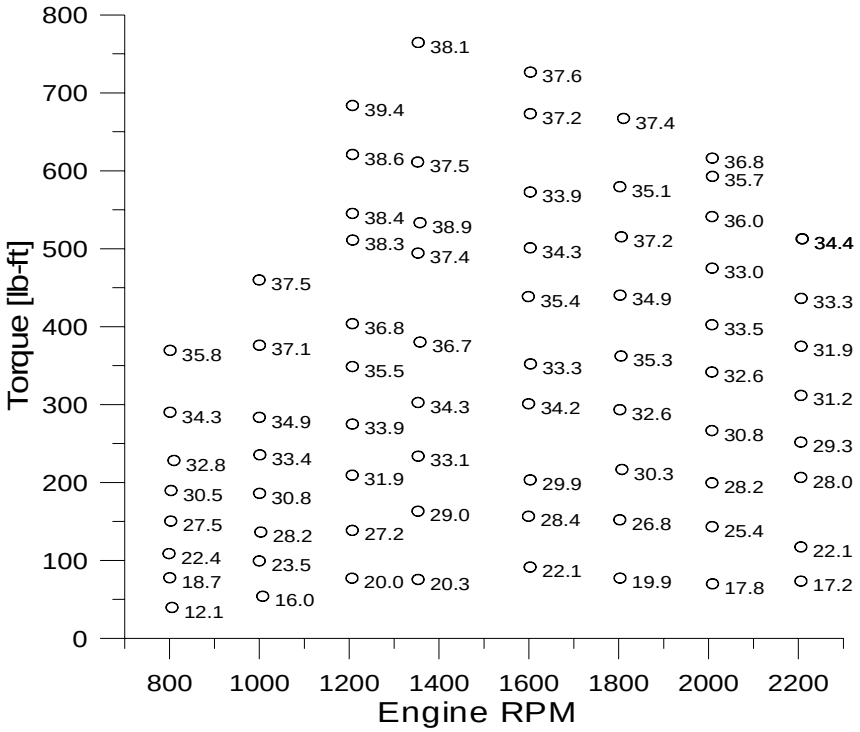


Figure 3. HCNG Brake Thermal Efficiency (LHV)

Figures 4 and 5 show the $NO_X$ emissions, in g/bhph, as a function of engine torque and rpm for the OEM CNG configuration and the converted HCNG configuration respectively.

Figures 2 and 3 show that the engine brake thermal efficiency is nearly identical between the OEM CNG and HCNG configurations at engine speeds above about 1300 rpm. Below that speed the HCNG efficiencies are slightly higher.

Comparing Figures 4 and 5 clearly shows that advantages of lean burn utilizing HCNG. Some operating conditions show almost a factor of 80 decrease in brake specific $NO_X$ emissions. Figure 4 shows the compromise in $NO_X$ emissions that had to be made to achieve equivalent engine torque at low rpm. For example, $NO_X$ emissions increase from well below 1 to nearly 3 g/bhph to achieve 770 ft-lbs of torque at 1350 rpm. Also, the maximum torque achieved by the HCNG configuration at 2200 rpm is reduced by about 20% when compared to the OEM CNG configuration. This was due to excessive air charge temperature for the aftermarket turbocharger chosen.

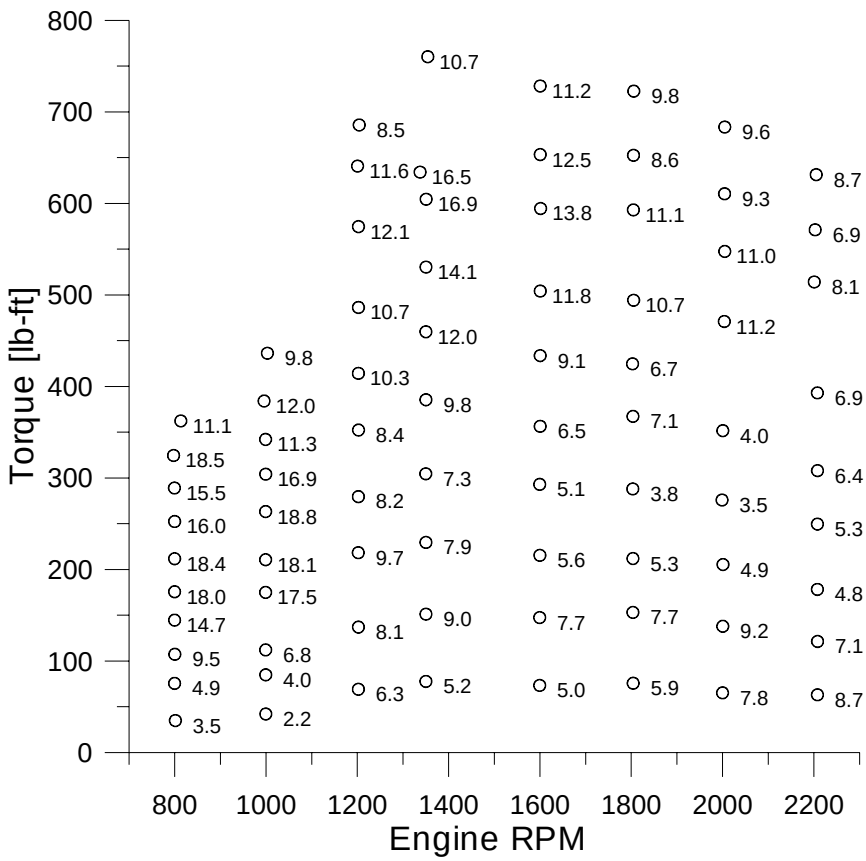


Figure 4. CNG Brake Specific $NO_X$ (g/bhph)

The $NO_X$ results from Figures 4 and 5 are further corroborated by the results of Tables 3 and 4. The simulated driving cycle $NO_X$ emissions are reduced by about 82% for HCNG. A major anomaly is the idle condition for both $NO_X$ and total hydrocarbon emissions. Clearly, this is an area where improved engine control with the aftermarket engine controller is needed.

A dramatic decrease in engine-out $NO_X$ emissions has been achieved using HCNG and lean burn. However, relying on engine components designed for different fuels and operating conditions limits the full capabilities of the technology. Namely, the cylinder heads and manifold designs for production natural gas engines are not compatible with the large air flows required by HCNG for ultimate $NO_X$ reductions. If the full potential of HCNG technology is to be realized, these components must be redesigned.

Results from the Phase II engine testing are shown in Table 1. Modifications in phase II were able to reduce $NO_X$ below the CARB 2007 standards. The highest $NO_X$ emissions are at high speed and high torque. The greatest emissions values are 0.16 g/bhph. The vast majority of torque-speed points show $NO_X$ emissions below 0.1 g/bhph. This data represents a factor of 40 reduction from the 2003 standard of 4.0 g/bhph. The brake specific fuel economy values show a slight reduction of a few percentage points in efficiency for peak power points.

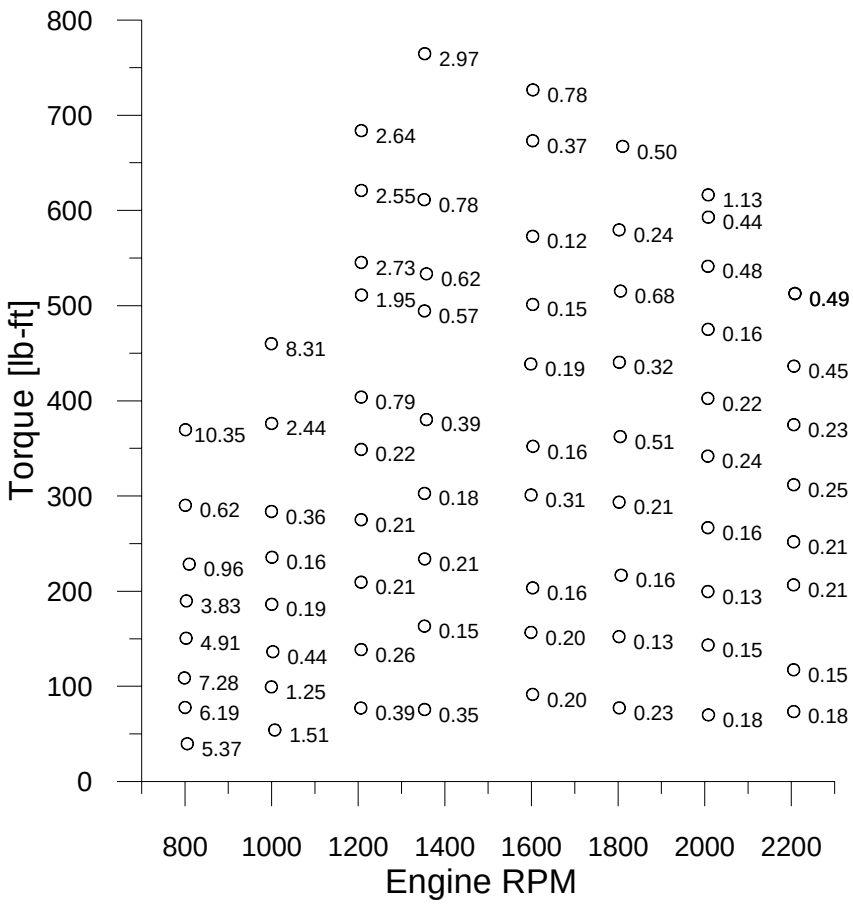


Figure 5. HCNG Brake Specific $NO_X$ (g/bhph)

The HCNG bus was tested in Reno, NA and Davis, CA. Figure 6 shows a picture of the bus. The bus was test driven around the UC Davis campus and has been used for several special events to ferry people around. Acceleration tests (see Table 2) showed that conventional CNG buses have better acceleration and drivers confirmed that result. This result was expected based on the dynamometer testing. Since acceleration is an important parameter for transit buses, Collier Technologies has designed the commercial prototype such that the acceleration of the

HCNG engine will be similar to that of conventional CNG buses. Further testing is necessary to determine whether maintenance of HCNG buses will differ from CNG buses.

Table 2. Acceleration testing of the CNG and HCNG buses. The Table shows average times to accelerate from rest to the final speed of 20 and 30 mph.

| Final Speed | CNG Bus Time (secs) | HCNG Time (secs) |
|---|---|---|
| 20 mph | 8.87 | 11.21 |
| 30 mph | 12.03 | 19.45 |

Overall, the Phase II modifications show that HCNG technology can meet the CARB 2007 standards. There were specific problems using the John Deere 8.1 liter engine which did not allow both meeting the standards and not sacrificing engine power. Results from the ICAT testing were instrumental for Collier Technologies in understanding how to proceed with a commercial prototype engine suitable or transit buses.

Collier Technologies has chosen the Daewoo 11.0 liter CNG engine to use as their commercial HCNG engine platform. The Daewoo engine is rated at 286 hp at 2200 rpm and 831 ft-lbs at 1320 rpm. That engine will be used in Phase III of the bus program. Modifications to the engine included engine timing adjustments, enhanced air flow capability, and operating at an equivalence ratio of roughly 0.53. Collier Technologies has tested the modified engine on their dynamometer. Results are shown in table 3.

Table 3. Results from Phase II engine dynamometer testing.

| Speed | Torque | CO | $NO_X$ | THC | Eff | Speed | Torque | CO | $NO_X$ | THC | Eff |
|---|---|---|---|---|---|---|---|---|---|---|---|
| (RPM) | Lb/ft | g/bhph | g/bhph | g/bhph | | (RPM) | Lb/ft | g/bhph | g/bhph | g/bhph | |
| 800 | 259 | 1.69 | 0.09 | 2.60 | 0.30 | 1400 | 512 | 1.21 | 0.12 | 1.32 | 0.33 |
| | 237 | 1.68 | 0.08 | 1.93 | 0.30 | | 469 | 1.21 | 0.10 | 1.39 | 0.33 |
| | 208 | 1.84 | 0.06 | 1.91 | 0.27 | | 409 | 1.26 | 0.09 | 1.45 | 0.33 |
| | 181 | 2.08 | 0.05 | 2.01 | 0.25 | | 356 | 1.33 | 0.09 | 1.46 | 0.32 |
| | 153 | 2.45 | 0.04 | 2.56 | 0.23 | | 309 | 1.43 | 0.08 | 1.45 | 0.31 |
| | 128 | 2.98 | 0.04 | 3.31 | 0.20 | | 259 | 1.46 | 0.08 | 1.30 | 0.31 |
| | 102 | 3.43 | 0.04 | 4.08 | 0.21 | | 212 | 1.59 | 0.07 | 1.32 | 0.30 |
| | 78 | 4.37 | 0.04 | 5.25 | 0.18 | | 157 | 2.02 | 0.06 | 1.65 | 0.26 |
| | 48 | 8.33 | 0.04 | 12.32 | 0.13 | | 108 | 2.42 | 0.06 | 1.93 | 0.24 |
| | 25 | 14.10 | 0.06 | 18.58 | 0.09 | | 59 | 4.09 | 0.06 | 3.23 | 0.17 |
| 900 | 283 | 1.60 | 0.08 | 2.35 | 0.30 | 1600 | 516 | 1.08 | 0.11 | 1.21 | 0.34 |
| | 259 | 1.66 | 0.07 | 2.15 | 0.30 | | 460 | 1.15 | 0.11 | 1.29 | 0.33 |
| | 231 | 1.76 | 0.07 | 2.04 | 0.29 | | 404 | 1.24 | 0.09 | 1.38 | 0.33 |
| | 200 | 1.98 | 0.06 | 2.09 | 0.28 | | 358 | 1.34 | 0.09 | 1.42 | 0.32 |
| | 175 | 2.17 | 0.05 | 2.34 | 0.26 | | 308 | 1.44 | 0.08 | 1.39 | 0.31 |
| | 141 | 2.60 | 0.04 | 2.84 | 0.24 | | 260 | 1.51 | 0.07 | 1.35 | 0.30 |
| | 118 | 3.08 | 0.04 | 3.73 | 0.22 | | 203 | 1.64 | 0.06 | 1.34 | 0.28 |
| | 88 | 3.92 | 0.04 | 5.20 | 0.19 | | 157 | 1.87 | 0.06 | 1.69 | 0.27 |
| | 58 | 5.62 | 0.04 | 6.81 | 0.15 | | 102 | 2.43 | 0.06 | 2.11 | 0.22 |
| | 30 | 9.95 | 0.05 | 12.62 | 0.10 | | 56 | 3.80 | 0.07 | 3.58 | 0.17 |
| 1000 | 314 | 1.56 | 0.08 | 2.49 | 0.31 | 1800 | 526 | 1.07 | 0.13 | 1.19 | 0.34 |
| | 284 | 1.69 | 0.08 | 2.55 | 0.31 | | 474 | 1.07 | 0.12 | 1.15 | 0.34 |
| | 256 | 1.79 | 0.08 | 2.33 | 0.30 | | 421 | 1.17 | 0.11 | 1.23 | 0.33 |
| | 218 | 1.92 | 0.07 | 2.71 | 0.29 | | 369 | 1.27 | 0.09 | 1.33 | 0.32 |
| | 188 | 2.10 | 0.06 | 3.35 | 0.27 | | 315 | 1.39 | 0.08 | 1.39 | 0.31 |
| | 156 | 2.47 | 0.05 | 3.90 | 0.25 | | 276 | 1.52 | 0.07 | 1.54 | 0.30 |
| | 125 | 3.14 | 0.05 | 4.18 | 0.22 | | 210 | 1.45 | 0.08 | 1.47 | 0.30 |
| | 92 | 3.91 | 0.04 | 6.39 | 0.20 | | 159 | 1.63 | 0.08 | 1.69 | 0.28 |
| | 68 | 5.42 | 0.04 | 3.41 | 0.17 | | 109 | 2.17 | 0.08 | 2.30 | 0.24 |
| | 37 | 12.75 | 0.06 | 5.44 | 0.10 | | 55 | 3.92 | 0.07 | 3.82 | 0.17 |
| 1200 | 437 | 1.60 | 0.08 | 2.82 | 0.32 | 2000 | 533 | 1.09 | 0.16 | 1.33 | 0.35 |
| | 407 | 1.45 | 0.10 | 1.58 | 0.32 | | 481 | 1.08 | 0.15 | 1.30 | 0.35 |
| | 353 | 1.46 | 0.10 | 1.84 | 0.32 | | 422 | 1.11 | 0.13 | 1.28 | 0.34 |
| | 304 | 1.54 | 0.09 | 2.15 | 0.31 | | 370 | 1.21 | 0.11 | 1.41 | 0.33 |
| | 264 | 1.68 | 0.08 | 2.77 | 0.30 | | 322 | 1.36 | 0.09 | 1.61 | 0.32 |
| | 217 | 1.96 | 0.07 | 3.32 | 0.29 | | 269 | 1.52 | 0.08 | 1.75 | 0.31 |
| | 178 | 2.26 | 0.06 | 5.96 | 0.27 | | 219 | 1.65 | 0.07 | 1.85 | 0.29 |
| | 136 | 2.79 | 0.05 | 6.98 | 0.24 | | 157 | 1.69 | 0.08 | 1.80 | 0.27 |
| | 97 | 3.86 | 0.04 | 3.07 | 0.20 | | 117 | 2.02 | 0.09 | 2.28 | 0.24 |
| | 40 | 5.34 | 0.10 | 4.59 | 0.12 | | 55 | 3.88 | 0.09 | 4.19 | 0.16 |
| 1350 | 515 | 1.60 | 0.11 | 2.79 | 0.33 | 2200 | 508 | 1.12 | 0.16 | 1.39 | 0.34 |
| | 489 | 1.57 | 0.09 | 1.63 | 0.35 | | 460 | 1.13 | 0.16 | 1.40 | 0.34 |
| | 421 | 1.46 | 0.10 | 1.88 | 0.33 | | 406 | 1.18 | 0.14 | 1.42 | 0.33 |
| | 362 | 1.54 | 0.10 | 2.11 | 0.32 | | 358 | 1.23 | 0.12 | 1.44 | 0.32 |
| | 312 | 1.63 | 0.09 | 2.62 | 0.31 | | 304 | 1.37 | 0.10 | 1.64 | 0.31 |
| | 261 | 1.72 | 0.08 | 3.26 | 0.30 | | 255 | 1.56 | 0.09 | 1.82 | 0.29 |
| | 208 | 1.96 | 0.07 | 3.82 | 0.28 | | 204 | 1.71 | 0.08 | 1.94 | 0.27 |
| | 156 | 2.20 | 0.06 | 5.27 | 0.27 | | 155 | 1.79 | 0.09 | 2.00 | 0.26 |
| | 106 | 2.47 | 0.07 | 4.77 | 0.23 | | 100 | 2.31 | 0.09 | 2.59 | 0.22 |
| | 55 | 3.63 | 0.09 | 5.90 | 0.17 | | 53 | 4.23 | 0.10 | 4.49 | 0.15 |

Table 4. Emissions and fuel economy for the Daewoo 11.0 liter HCNG engine.

| Speed | Torque | CO | $NO_X$ | THC | Eff | Speed | Torque | CO | $NO_X$ | THC | Eff |
|---|---|---|---|---|---|---|---|---|---|---|---|
| (RPM) | Lb/ft | g/bhph | g/bhph | g/bhph | | (RPM) | Lb/ft | g/bhph | g/bhph | g/bhph | |
| 800 | 340 | 1.12 | 0.08 | 1.29 | 0.33 | 1400 | 736 | 1.08 | 0.08 | 1.44 | 0.35 |
| | 305 | 0.85 | 0.09 | 1.28 | 0.33 | | 669 | 0.59 | 0.09 | 1.32 | 0.35 |
| | 268 | 0.89 | 0.08 | 1.26 | 0.31 | | 582 | 0.59 | 0.09 | 1.29 | 0.35 |
| | 234 | 0.98 | 0.07 | 1.40 | 0.30 | | 533 | 0.59 | 0.09 | 1.25 | 0.34 |
| | 199 | 1.16 | 0.06 | 1.61 | 0.28 | | 445 | 0.61 | 0.09 | 1.20 | 0.34 |
| | 168 | 1.38 | 0.05 | 1.92 | 0.26 | | 365 | 0.66 | 0.08 | 1.24 | 0.32 |
| | 136 | 1.75 | 0.05 | 2.29 | 0.24 | | 303 | 0.71 | 0.07 | 1.33 | 0.31 |
| | 99 | 2.46 | 0.04 | 3.07 | 0.20 | | 223 | 0.83 | 0.07 | 1.51 | 0.28 |
| | 72 | 3.23 | 0.04 | 4.29 | 0.17 | | 146 | 1.07 | 0.07 | 1.75 | 0.24 |
| | 39 | 5.32 | 0.05 | 7.20 | 0.11 | | 79 | 1.86 | 0.08 | 2.86 | 0.17 |
| 900 | 373 | 1.18 | 0.07 | 1.58 | 0.33 | 1600 | 719 | 1.09 | 0.08 | 1.31 | 0.34 |
| | 282 | 1.04 | 0.08 | 1.36 | 0.32 | | 650 | 0.59 | 0.10 | 1.13 | 0.35 |
| | 307 | 1.03 | 0.09 | 1.38 | 0.33 | | 572 | 0.59 | 0.10 | 1.13 | 0.34 |
| | 235 | 1.14 | 0.07 | 1.46 | 0.30 | | 512 | 0.60 | 0.09 | 1.07 | 0.34 |
| | 208 | 1.25 | 0.07 | 1.63 | 0.29 | | 442 | 0.61 | 0.09 | 1.08 | 0.33 |
| | 171 | 1.47 | 0.06 | 1.87 | 0.27 | | 358 | 0.63 | 0.09 | 1.11 | 0.31 |
| | 132 | 1.91 | 0.06 | 2.26 | 0.24 | | 284 | 0.72 | 0.08 | 1.29 | 0.3 |
| | 100 | 2.51 | 0.06 | 2.82 | 0.21 | | 219 | 0.86 | 0.08 | 1.72 | 0.28 |
| | 67 | 3.80 | 0.05 | 3.95 | 0.17 | | 142 | 1.10 | 0.08 | 1.97 | 0.23 |
| | 30 | 7.17 | 0.09 | 7.70 | 0.09 | | 65 | 2.29 | 0.09 | 3.61 | 0.15 |
| 1000 | 414 | 1.11 | 0.08 | 1.51 | 0.34 | 1800 | 669 | 1.57 | 0.08 | 1.70 | 0.33 |
| | 313 | 1.02 | 0.08 | 1.30 | 0.33 | | 600 | 0.61 | 0.11 | 1.13 | 0.34 |
| | 283 | 1.03 | 0.08 | 1.30 | 0.32 | | 532 | 0.61 | 0.10 | 1.09 | 0.33 |
| | 239 | 1.09 | 0.07 | 1.39 | 0.31 | | 467 | 0.63 | 0.09 | 1.07 | 0.32 |
| | 205 | 1.24 | 0.06 | 1.55 | 0.29 | | 420 | 0.65 | 0.09 | 1.20 | 0.31 |
| | 170 | 1.42 | 0.06 | 1.81 | 0.27 | | 341 | 0.68 | 0.09 | 1.08 | 0.3 |
| | 137 | 1.80 | 0.06 | 2.10 | 0.25 | | 271 | 0.76 | 0.09 | 1.24 | 0.28 |
| | 108 | 2.26 | 0.05 | 2.50 | 0.22 | | 195 | 0.95 | 0.09 | 1.81 | 0.26 |
| | 71 | 3.41 | 0.06 | 3.55 | 0.17 | | 132 | 1.23 | 0.09 | 2.24 | 0.22 |
| | 38 | 5.80 | 0.07 | 5.55 | 0.11 | | 72 | 2.15 | 0.10 | 3.33 | 0.15 |
| 1200 | 745 | 1.06 | 0.08 | 1.49 | 0.35 | 2000 | 614 | 1.26 | 0.11 | 1.40 | 0.32 |
| | 675 | 0.60 | 0.08 | 1.33 | 0.35 | | 535 | 1.19 | 0.09 | 1.29 | 0.31 |
| | 602 | 0.60 | 0.08 | 1.32 | 0.35 | | 501 | 1.26 | 0.08 | 1.28 | 0.3 |
| | 532 | 0.62 | 0.08 | 1.27 | 0.34 | | 443 | 1.36 | 0.07 | 1.27 | 0.29 |
| | 448 | 0.61 | 0.08 | 1.24 | 0.33 | | 381 | 1.31 | 0.07 | 1.14 | 0.28 |
| | 370 | 0.65 | 0.08 | 1.24 | 0.32 | | 314 | 1.32 | 0.07 | 1.12 | 0.27 |
| | 295 | 0.71 | 0.07 | 1.36 | 0.3 | | 255 | 1.46 | 0.07 | 1.21 | 0.25 |
| | 219 | 0.84 | 0.07 | 1.52 | 0.28 | | 202 | 1.67 | 0.07 | 1.38 | 0.24 |
| | 151 | 1.03 | 0.08 | 1.76 | 0.24 | | 119 | 2.35 | 0.09 | 2.22 | 0.19 |
| | 82 | 1.82 | 0.07 | 2.86 | 0.18 | | 68 | 3.67 | 0.11 | 3.16 | 0.13 |
| 1350 | 745 | 1.06 | 0.08 | 1.49 | 0.35 | 2200 | 577 | 0.92 | 0.14 | 1.53 | 0.31 |
| | 675 | 0.60 | 0.08 | 1.33 | 0.35 | | 283 | 1.53 | 0.09 | 1.40 | 0.26 |
| | 602 | 0.60 | 0.08 | 1.32 | 0.35 | | 231 | 1.50 | 0.09 | 1.43 | 0.24 |
| | 532 | 0.62 | 0.08 | 1.27 | 0.34 | | 190 | 1.65 | 0.10 | 1.60 | 0.23 |
| | 448 | 0.61 | 0.08 | 1.24 | 0.33 | | 132 | 2.24 | 0.10 | 2.03 | 0.19 |
| | 370 | 0.65 | 0.08 | 1.24 | 0.32 | | 70 | 3.53 | 0.12 | 3.03 | 0.13 |
| | 295 | 0.71 | 0.07 | 1.36 | 0.3 | | | | | | |
| | 219 | 0.84 | 0.07 | 1.52 | 0.28 | | | | | | |
| | 151 | 1.03 | 0.08 | 1.76 | 0.24 | | | | | | |
| | 82 | 1.82 | 0.07 | 2.86 | 0.18 | | | | | | |

Figure 6. The HCNG bus.

### 3.3 HCNG combustion modeling

An engine model with detailed chemical reactions was developed to predict the "in cylinder" production to $NO_X$ under realistic engine conditions. The model consists of the following four parts: (1) A simplified engine model to predict the "in cylinder" maximum pressure for $CH_4/H_2$ mixtures; (2) A semi-empirical model to predict the detailed pressure and fuel rate curves during an engine cycle, which is based on achieving MBT (maximum brake torque – the torque that has the highest efficiency at a given engine speed); (3) A detailed flame structure model to predict $NO_X$ formation during the engine cycle with the use of GRI chemical reaction mechanism; and (4) A detailed chemical model to predict the influence of "in cylinder" compression and expansion on the evolution of the different burned gas parcels in the engine. The model has been applied to the entire engine cycle from the inlet to the exhaust processes. The results include a wide range of lean equivalence ratio studies with excellent agreement with the limited experimental results.

The general features and major conclusions of the modeling are the following:

- The model applies the GRI 3.0 chemical kinetic mechanism to the combustion process, and it takes into account detailed local flame structure, and the variation of $NO_X$ due to compression and expansion of the products of combustion.
- The model neglects the influence of mixing of combustion products after combustion, as well as the influence of turbulence on flame structure.
- Simulations of $CH_4$ and $CH_4/H_2$ mixtures have yielded $NO_X$ values that are typical seen in the field. This is true over a range of equivalence ratios that range from stoichimetric to very lean.
- The model predicts that lean mixtures of $CH_4$ and $H_2$ can produce very low values of $NO_X$.
- The results indicated that there is high sensitivity of $NO_X$ to equivalence ratio. For example, the variation in $NO_X$ between equivalence ratios of 0.7 and 0.6 can vary by almost and order of magnitude.

An SAE paper was written describing the model and the results. The paper title is "Analysis and Prediction of in Cylinder $NO_X$ Emissions for Lean Burn CNG/$H_2$ Transit Bus Engines". The paper is included with this report.

### 3.4 Transit bus simulations

In order to predict the improvement in $NO_X$ emissions for bus driving cycles, vehicle simulations was performed using ADVISOR. A Neoplan bus vehicle file was created from the 2 engine maps with emission data provided above, and from the following ADVISOR vehicle components: a 5-speed heavy-duty transmission (ZFHP590AT), heavy-duty wheel-axle, heavy-duty accessories, powertrain control PTC_CONVAT5spd. The mass of the bus was 17091.4 kg.

The two buses were simulated driving the Central Business (CBD14), New York Bus (NYB), and New York City Composite (NYCCOMP) driving cycles. The CBD14 driving cycle attempts to simulate stop and go behavior of transit busses by accelerating to 20 mph, holding for a few seconds, the decelerating to 0, idling for a few seconds, and then repeats 13 more times. The NYB cycle models the driving cycle of a heavy duty truck or transit bus in New York City. The NYB driving cycle has long idle times; short spurts of steep acceleration/decelerations, and has a maximum speed of 30 mph. The NYCCOMP driving cycle is the most rigorous of the three, requiring the hardest acceleration and decelerations, but spends a relatively short time idling. Figures 7-9 show plots of the 3 drive cycles showing speed versus time.

Engine maps for fuel use and emissions (HC, CO, and $NO_X$) were input into ADVISOR. The maps are indexed horizontally by torque, 75, 150, 225, 300, 375, 450, 525, 600, 675, 750 lb-ft.; and vertically by speed, 800, 1000, 1200, 1350, 1600, 1800, 2000, 2200 rpm. For each second of simulation, emissions and fuel use are linearly extrapolated within the map at the engine's operating point. While ADVISOR supports multiple temperature maps and particulate matter (PM) emissions, the maps we entered were for hot steady state engine conditions, and we had no particulate matter emissions data. Advisor does not model (nor do we have data for) transient emissions.

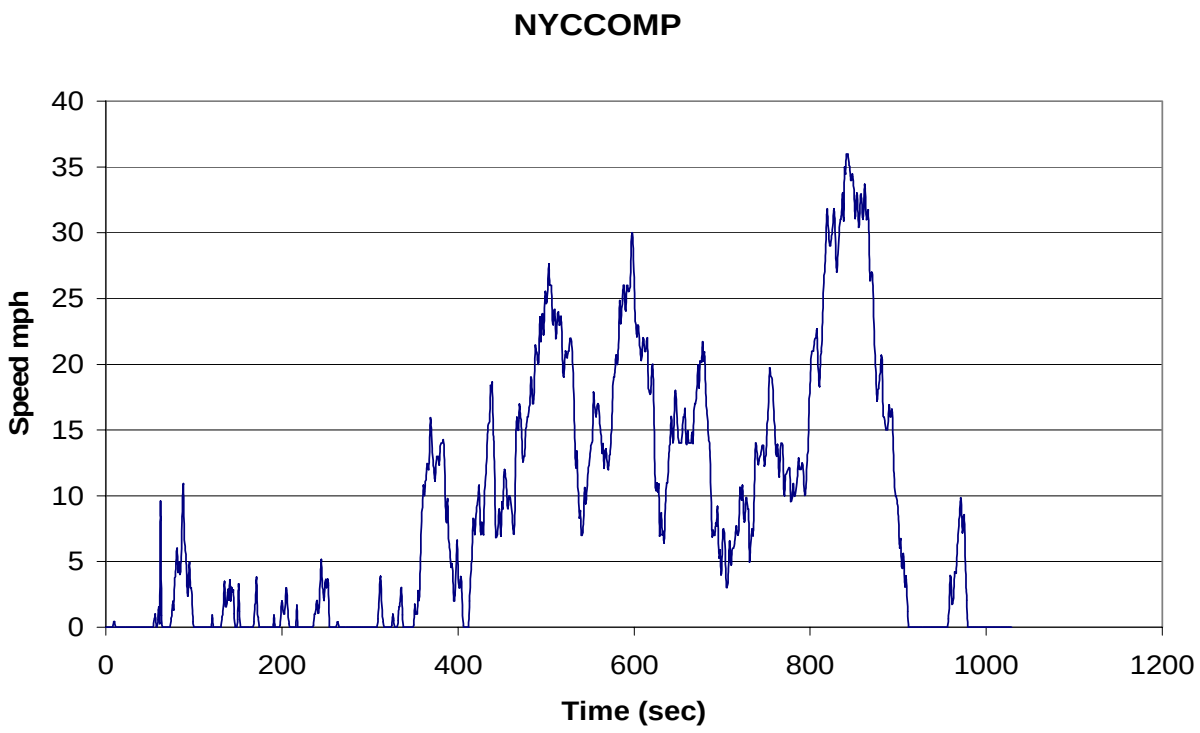


Figure 7. Speed versus time for the NYCCOMP drive cycle.

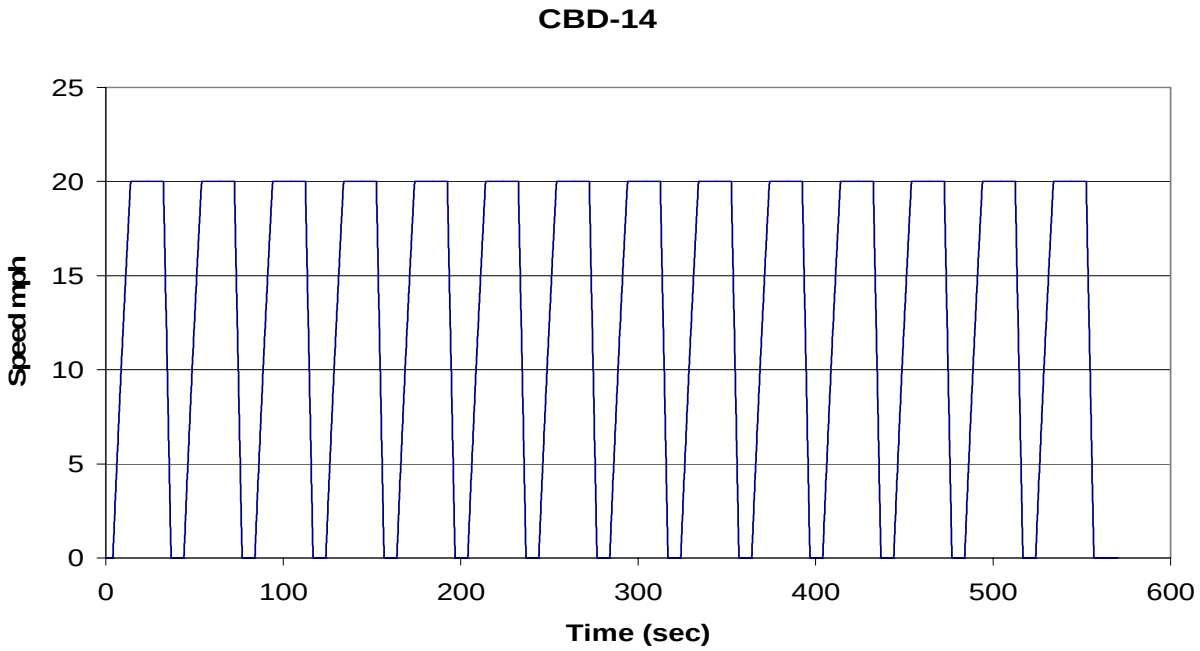


Figure 8. Speed versus time for the CBD14 drive cycle.

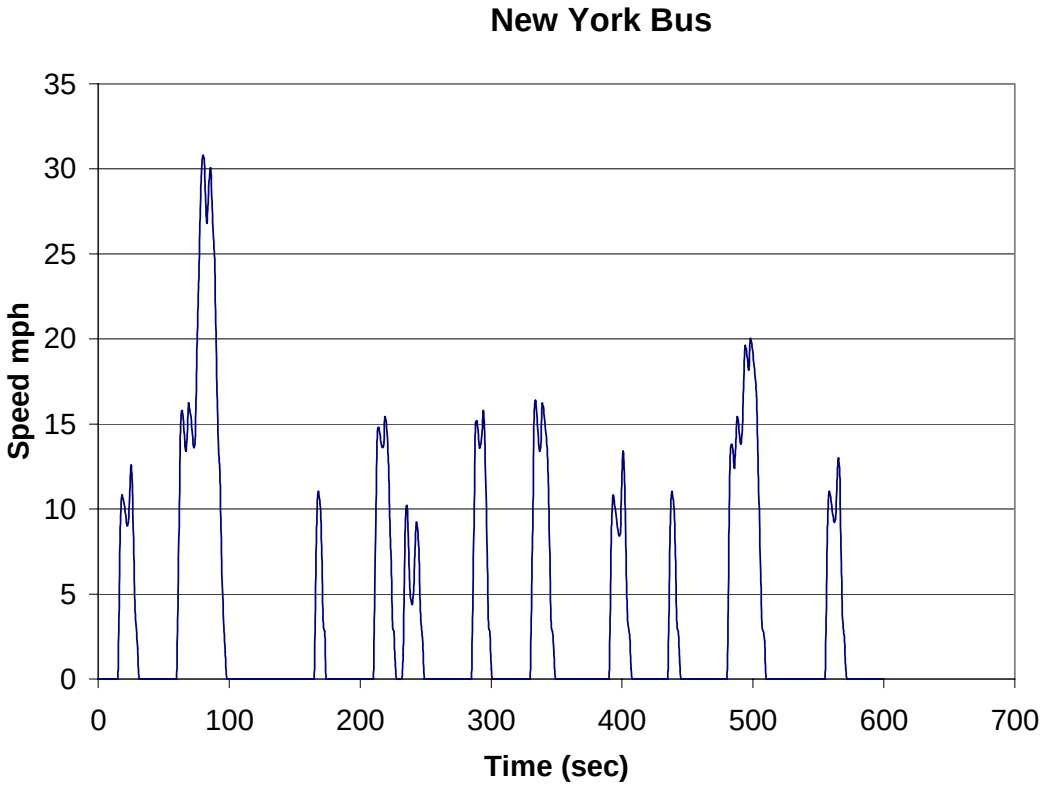


Figure 9. Speed versus time for the New York Bus drive cycle.

Advisor calculates engine torque and speed on a second by second basis. Given the bus speed at time, t, and the speed one second later, t + 1, Advisor calculates the engine power, speed, and torque necessary to accelerate or decelerate the bus to the appropriate speed in that second. The torque and speed values are considered fixed for that second. Advisor determines the fuel economy and emissions by interpolating the torque and speed in lookup tables. The data in these fuel economy and emissions lookup tables were taken during steady state operation.

Table 5 shows the results ADVISOR produced after running each of the 2 bus models with Phase I data. Emissions data for the drive cycles is presented in units of grams per mile, and fuel economy in miles per diesel equivalent. The results show the HCNG bus achieves about 85% reduction in $NO_X$, and a significant increase in HC and CO emissions in comparison with the stock CNG bus. The HCNG bus is a little more fuel efficient, but probably at the expense of a little less power. Neither of the busses was able to meet all of the drive cycles, as some of the drive cycles acceleration requests were greater than what the engines could produce.

### 3.5 Commercialization Costs

HCNG Vehicle Cost Analysis

HCNG buses require only modifications to the engine in order to reduce $NO_X$ emissions below the CARB 2007 standards. Hydrocarbons emissions will require after treatment with a standard 2 way catalyst. Thus, the only cost considerations are those relevant to the engine

modifications and a catalyst. There are three ways the engine modifications could be made. First, stock CNG engines could be retrofitted with hardware and appropriate control software to run on HCNG fuel. Second, the stock engine could be replaced with another engine designed to run on HCNG fuel. Finally, the engine manufacturers could design their stock engines for HCNG fuel. The first two methods would allow transit agencies to retrofit for HCNG operation any CNG bus currently in service. The last method would apply to new buses. Each option will be discussed below.

Table 5. Results from Advisor simulations of CNG and HCNG buses. MPGDE = miles per gallon of diesel equivalent.

| | **HC (g/mi)** | **CO (g/mi)** | **$NO_X$ (g/mi)** | **MPGDE** |
|---|---|---|---|---|
| **CBD14** | | | | |
| CNG bus | 21.08 | 1.15 | 70.15 | 2.70 |
| HCNG bus | 23.34 | 7.36 | 6.58 | 3.18 |
| Change | 2.225 | 6.21 | -63.57 | 0.4 |
| **NYB** | | | | |
| CNG bus | 52.04 | 3.344 | 248.99 | 0.82 |
| HCNG bus | 95.64 | 20.52 | 36.35 | 1.06 |
| Change | 43.59 | 17.17 | -212.64 | 0.2 |
| **NYCCOMP** | | | | |
| CNG bus | 24.24 | 1.378 | 98.94 | 2.0 |
| HCNG bus | 35.77 | 8.45 | 14.21 | 2.59 |
| Change | 11.53 | 7.08 | -84.73 | 0.5 |

The first option is considered much less desirable than the other two. Current CNG engines were generally taken from diesel designs and are not ideal for running on HCNG fuel. In general, the R&D cost to understand how to modify these engines plus the cost of those modifications will be high compared to the cost of the other options.

Collier Technologies has worked with Daewoo to design an 11.0 liter HCNG engine capable of meeting the CARB 2007 $NO_X$ standards. This engine could replace a stock CNG engine in transit buses. Collier Technologies has estimated that the cost for delivery of the Daewoo HCNG engine would be roughly $40,000. That cost would not include installation or removal of the stock engine.

There are several considerations relevant to costing stock HCNG engines. In theory, engine manufacturers could work with Collier Technologies to understand how to redesign their CNG engines for HCNG operation. Once the modifications were understood, the manufacturers would modify their production facility to produce the new designs. The new engines would not require any new components or materials from those in their CNG engine designs. The new HCNG engines would then cost roughly the same to manufacture as conventional CNG engines. The manufacturers would, however, have to build new tooling facilities, and therefore, would incur some significant capital costs to proceed. Whether this capital cost should increase the price of stock engines in transit buses is not clear. Collier Technologies has estimated the overall R&D costs for engine modifications at roughly $200,000. In addition, Collier Technologies would include a licensing fee of $2,500/engine for the new HCNG engines. Assuming that a

large number of stock HCNG engines were produced, the incremental cost per engine would be very low compared to bus costs. For 1000 produced engines, the cost would be less than $5,000.

HCNG Fueling Station Cost Analysis

HCNG buses require both natural gas and hydrogen infrastructure for fueling. Transit agencies that currently run CNG buses already have the necessary natural gas hardware and would only require the addition of hydrogen infrastructure for a HCNG fueling facility. Those agencies that do not run CNG buses would need to install equipment for both natural gas and hydrogen. It seems likely that the first adopters of HCNG buses will be transit agencies that already have natural gas buses. The economic analysis described below will only address the necessary costs of adding hydrogen infrastructure to an existing natural gas facility.

The type and cost of hydrogen infrastructure necessary to support a fleet of HCNG buses depends on the fleet size. Small fleets do not require as much hydrogen and can use simpler stations. As the fleets grow, the hardware must supply more hydrogen, and the costs grow. The analysis below shows estimates for 2 HCNG fleets sizes: 100 kg $H_2$/day and 1000 kg $H_2$/day. These station sizes are suitable for 10 and 100 HCNG buses respectively.

The basic requirements needed to add hydrogen to existing natural gas stations are hydrogen production and storage, a compressor, buffer storage, and blending hardware. Some stations could have hydrogen brought to the facility in liquid hydrogen tankers or in hydrogen tube trailers. Other stations would have the hydrogen produced on-site by natural gas reformers or water electrolysers. The hydrogen must be compressed to pressures above the nominal 3600 psi fueling pressure. Since most compressors do not compress the fuel directly onto the vehicle, there must be some buffer storage to store the compressed hydrogen before mixing. A blend unit mixes the compressed hydrogen with compressed natural gas before dispensing the HCNG fuel onto buses.

The cost model includes capital costs for hardware, installation costs, and operating costs including fuel (for example, natural gas for stations with reformers). Costs are near to midterm costs (0-5 years roughly). Table 3 shows the costs broken down into hardware, installation, contingency, energy, and fixed operating costs. The total capital cost and the annual operating cost is shown. Finally, the overall cost is given as an annual cost over the lifetime of the station, and the cost for hydrogen dispensed is shown in $/kg.

These costs would have to be added to the current depreciated capital and operating costs of the agencies natural gas station. While the cost of the larger station is significantly higher, the cost for hydrogen dispensed is less than half of the smaller station cost. These costs are expected to drop as hydrogen demand increases. Estimated hydrogen demand for transit buses is discussed in the next section, but the main increase in demand is expected to come from the introduction of light duty hydrogen fuel cell vehicles. The timeframe for introduction is unclear but demand is very likely to be insignificant over the next 10-15 years.

Table 6. Estimated costs for hydrogen infrastructure for fleets of HCNG buses.

| Station 1: Steam Methane Reformer, 100 kg/day (10 buses) | | | |
|---|---|---|---|
| | | $ | $/yr |
| Natural gas reformer | 18.1% | $317,981 | |
| Purifier | 3.6% | $63,715 | |
| Storage System | 11.2% | $196,865 | |
| Compressor | 2.9% | $51,652 | |
| Dispenser | 2.4% | $42,377 | |
| Additional Equipment | 4.1% | $72,098 | |
| Installation Costs | 11.4% | $193,455 | |
| Contingency | 6.3% | $109,784 | |
| Natural gas | 8.6% | | $19,708 |
| Electricity costs (energy + demand) | 2.7% | | $6,289 |
| Fixed Operating Costs | 28.9% | | $66,597 |
| Total | 100% | **$1,047,927** | **$92,594** |
| Annual Cost ($/yr) | $230,369 | | |
| Hydrogen Price ($/kg) | $13.30 | | |

| Station 2: Steam Methane Reformer, 1000 kg/day (100 buses) | | | |
|---|---|---|---|
| Natural gas reformer | 14.7% | $1,265,904 | |
| Purifier | 2.3% | $201,486 | |
| Storage System | 27.6% | $2,372,295 | |
| Compressor | 2.0% | $171,113 | |
| Dispenser | 1.5% | $127,130 | |
| Additional Equipment | 0.9% | $77,458 | |
| Installation Costs | 3.6% | $300,373 | |
| Contingency | 7.2% | $621,443 | |
| Natural gas | 17.4% | | $197,080 |
| Electriciy costs (energy + demand) | 5.6% | | $63,205 |
| Fixed Operating Costs | 17.3% | | $195,993 |
| Total | 100% | **$5,137,202** | **$456,278** |
| Annual Cost ($/yr) | $1,131,685 | | |
| Hydrogen Price ($/kg) | $6.53 | | |

## 4. Status of the Technology

Because the technology demonstrated by this project utilizes no new engine technology, the commercial readiness is quite close. However, this project has also demonstrated that merely changing fuels and the computer algorithms of the engine controller do not achieve the ultimate emissions results that the technology is capable of attaining. In order to keep the same power the air flow must be increased significantly.

The results of this project has shown that $NO_X$ reductions on the order of a factor of 5 are achievable by merely replacing fuel and computer algorithms, a factor of ten is required to meet

$NO_X$ requirements in the year 2007. The data from the John Deere engine modified for HCNG fuel meet the CARB standards, but the engine has reduced power. To reach the factor of 10 reductions one of two solutions can be utilized. First, the engine air system can be modified to deliver significantly more air through use of special turbochargers or superchargers. Second, the engine can be oversized then de-rated for power. Collier Technologies developed their present commercial prototype based on the information gained from the ICAT program. The commercial prototype uses a larger engine (Daewoo 11 liter) and enhanced air flow capability.

## 5. Updated Commercialization Plan

The knowledge obtained from this project has greatly assisted the commercialization of the technology. It has clearly shown us that merely modifying an existing engine platform with external modifications will not achieve the $NO_X$ emissions goals necessary to commercialize in California. As a result of this project, we are pursuing the use of an engine specifically designed for hydrogen-natural gas fuel mixtures for ultra-lean burn operation.

We have an agreement in place with Daewoo Heavy Industries to be the US distributor for their natural gas engine line. We are planning to sell engines that are jointly manufactured in South Korea and the US with engine components specially-designed for this technology. Preliminary results show that this approach does indeed achieve the factor of ten reduction in $NO_X$ emissions necessary to meet California's 2007 emissions requirement.

The new engine will be branded "City Engines". The short block will be made in South Korea with the remaining parts being manufactured in the US, including cylinder heads. We have begun recruiting distributors for the new engine. The interested candidates are currently Detroit Diesel distributors. Detroit Diesel has discontinued their supply and support for natural gas engines. This has created a void in both replacement and new bus engines as well as parts for existing engines.

We are now capable of supplying OEM engines for both repowering and new bus applications that will meet the anticipated new $NO_X$ emissions standards for 2007. It is this engine that we are proposing to UC Davis to be used in Phase III of their DOT funded development program.

# Appendix A. Combustion Paper

**Paper # 04SFL-35**

## Analysis and Prediction of in Cylinder NOx Emissions for Lean Burn CNG/H2 Transit Bus Engines

**Harry A. Dwyer, Zach McCaffrey, Marshall Miller**
Institute of Transportation Studies, University of California, Davis

Copyright © 2004 SAE International

### ABSTRACT

In the immediate future the introduction of a wider variety of fuel types will play a significant role in reducing emissions and in solving the energy needs of the transportation industry. Both compressed natural gas, CNG, and hydrogen are expected to play significant roles, and the present paper shows that these fuels, when used together, can offer large benefits in NOx emissions. Significant reductions in NOx emissions will be required for CNG transit buses and heavy duty trucks, if they are to meet the future stringent emissions standards that come into effect in the year 2007.

In the present paper we have applied a newly developed engine model with detailed chemical reactions to predict the "in cylinder" production to NOx under realistic engine conditions. The model consists of the following four parts: (1) A simplified engine model to predict the "in cylinder" maximum pressure for CH4/H2 mixtures; (2) A semi-empirical model to predict the detailed pressure and fuel rate curves during an engine cycle, which is based on achieving MBT; (3) A detailed flame structure model to predict NOx formation during the engine cycle with the use of GRI chemical reaction mechanism; and (4) A detailed chemical model to predict the influence of "in cylinder" compression and expansion on the evolution of the different burned gas parcels in the engine. The model has been applied to the entire engine cycle from the inlet to the exhaust processes. The results include a wide range of lean equivalence ratio studies with excellent agreement with the limited experimental results, and the full paper will discuss the trade offs between NOx production, equivalence ratio, power, and inlet boost pressure.

### INTRODUCTION

During the last twenty years there has been considerable interest in the use of CNG and hydrogen fueled engines because of the potential reductions that can be obtained in engine emissions [1][2][3][4]. A recent paper by Collier, et al [5] has clearly shown that very low levels of NOx can be achieved for lean mixtures of H2 and CNG. The basic thesis of the present paper is that the superior combustion characteristics of hydrogen allow for the efficient combustion of very lean mixtures in an engine, and this leads to reduce temperatures in the engine. The influence of reduced temperatures on the finite rate production of NOx can be well described by the extended chemical reaction mechanism known as GRI-MECH 3.0, [6], and this approach has been used in the present research.

In order to obtain realistic modeling results for NOx in an engine a detailed model of the temperature and species in the engine as a function of time must be used, and in the present paper we have used a new semi-empirical model to predict NOx over a variety of power outputs and stoichiometries for natural gas and hydrogen. The model allows for the prediction of non-equilibrium chemical species as a function of crank angle. The present model also has the ability to treat more than one fuel, and this is a necessary feature for mixtures of hydrogen and CNG. The model is not as detailed as complex three-dimensional CFD studies, however it appears to be detailed enough to yield both quantitative and qualitative insight.

### MAIN SECTION

METHODS OF APPROACH – Although the model presented in this paper is not a fully time-dependent and three-dimensional model of an engine, it is a detailed time dependent description of the chemical rate processes in the

engine, and it does predict how NOx and other species vary with the changing pressures and temperatures in the engine. The model consists of four parts and they will now be described in detail.

The first part of the model is a sub-model that predicts the maximum cylinder pressure as a function of boast pressure, rpm, compression ratio, indicated mean effective pressure, and equivalence ratio. This sub-model computer code has been developed at UC Davis, and it is given the name CHEMK6 [7] [8]. For our present study the code was applied to a John Deere 8.1L 6081H CNG Engine, and a semi-empirical correction was applied to relate indicated mean effective pressure, IMEP, to brake mean effective pressure, BMEP. CHEMK6 has the capability to use fuel mixtures over a wide range of equivalence ratio, and it is based the use of CHEMKIN II, [11], which allows for variable thermo physical properties.

The second sub-model predicts a detailed pressure curve in the engine during the power stroke, and this pressure curve is related to the ignition and fuel consumption rates in the cylinder. Typical results form this sub-model are shown in Fig. 1, and they have been developed semi-empirically from the results in Heywood [9]. Before ignition the compression of the fuel air mixture is described by a $pv^n = \text{constant}$ process, and after ignition the burning rate has been adjusted for Maximum Brake Torque, MBT. After the combustion process has been completed, the products of combustion are expanded again with a $pv^n = \text{constant}$ process, and the exponent has been chosen to be 1.35 for compression and 1.27 for the expansion part of the power cycle. The consumption of fuel is typical of proper engine timing, and the burning process occurs over crank angles of 30º before Top Dead Center, TDC, and 50º after TDC, and this is typical of engines that have been tuned for MBT. This sub-model has been assembled with the use of MATLAB [12], and requires the input from the first sub-model, as well of the characteristics of the engine to be investigated.

The third sub-model consists of a time accurate flame code that predicts the detailed burning of the fuel mixture at a given crank angle in the engine. The flame code solves the equations of continuity, energy, and species transport that are appropriate for the GRI 3.0 reaction mechanism [6]. The specific control volume equations that are solved are the following

$$\frac{\partial}{\partial t}\iiint_V \rho dV + \iint_S \rho \vec{V} \cdot d\vec{A} = 0 \quad \text{Continuity}$$

$$\iiint_V \rho C_p \left[ \frac{\partial T}{\partial t} + u \frac{\partial T}{\partial x} \right] dV = \iint_A k \vec{\nabla} T \cdot d\vec{A} \quad \text{Energy}$$

$$-\iiint_V \rho \sum_{k=1}^{kk} Y_k C_{p,k} \vec{V}_k \cdot \vec{\nabla} T dV - \iiint_V \dot{\omega} h_k W_k dV$$

$$\iiint_V \rho \left[ \frac{\partial Y_k}{\partial t} + u \frac{\partial Y_k}{\partial x} \right] dV = -\iint_A \rho Y_k \vec{V}_k \cdot d\vec{A} \quad \text{Species}$$

$$+\iiint_V \dot{\omega}_k W_k dV$$

where the following notation has been used: $\rho$ -density, $V$ - volume, $A$ - area, $u$ - velocity, $T$ - temperature, $Y_k$ - mass fraction of species k, $C_p$ - specific heat, $\vec{V}_k$ - diffusion velocity of species k, $k$ - thermal conductivity, $\dot{\omega}_k$ - production of species k, and $W_k$ - molecular weight of species k.

In order to model the influences of compression of the unburned mixture in the engine, the flame is given the instantaneous pressure and temperature of the unburned mixture as a function of crank angle. Since the temperatures

and pressures in the engine can exceed 1000K and 70 atm in CNG engines, there is no steady state solution for mixtures under these conditions. Therefore, the flame structure must be calculated before there is time for spontaneous ignition. The method of solution of these equations is similar to Reference [13].

Typical results of a flame calculation are shown in Fig. 2, and this figure contains three axes, which are time, space and temperature, while the contour surface displays the levels of nitrous oxide, NO. At very early times the inflowing mixture of methane, CH4, and hydrogen, H2, and air is ignited by pure hot nitrogen. As the flame forms the gases used for ignition are convected out of the computation region, and the steep flame zone is captured with the use of an adaptive mesh procedure near the midpoint of the computational zone. The results shown in Fig. 2 have been obtained in a time less than a millisecond, and these results are typical for all of the cases shown in the paper.

The spatial distributions at the final time of a typical flame simulation are shown in Fig. 3, where temperature, NO, and nitrous dioxide, NO2, mass fractions are given (This figure is a slice of Fig.2). In the figure the sharp temperature rise in the flame is followed by a flat region, and at the end of the x axis, there is a small region of high temperature ignition fluid that has not passed out of the computational region. Both NO and NO2 increase in the flat temperature region, and this is due to the highly non-equilibrium nature of the chemical reactions associated with these species. However, in a realistic engine the pressure is changing and the NOx products must be subjected to this changing environment. In our study we have taking the first point in the flat temperature region as the input to the bomb model, where it evolves due to the changing engine cylinder conditions. There is no exact way of picking this spatial location, however our results are not very sensitive to the choice, and it appears physically reasonable from the results shown in Fig. 3.

The physical conditions in Fig. 2 correspond to a crank angle of 10 degrees after TDC, 2000 rpm, inlet pressure of 1.6 atm, inlet temperature of 340 K, a lean mixture of CH4 and H2 (33% H2) at an equivalence ratio of .6. The local unburned pressure and temperature of the mixture was 47.4 atm and 972 K, respectively. In order to obtain a complete simulation during the engine cycle, the flame structure was calculated every 2.5 or 5 degrees during fuel burning depending on engine conditions.

The final sub-model is used to take the flame products that have been created during the combustion process, and expand and compress them based on the variation of cylinder pressure. In this model we have assumed that there is no mixing between the various flame products that have been created during different parts of the

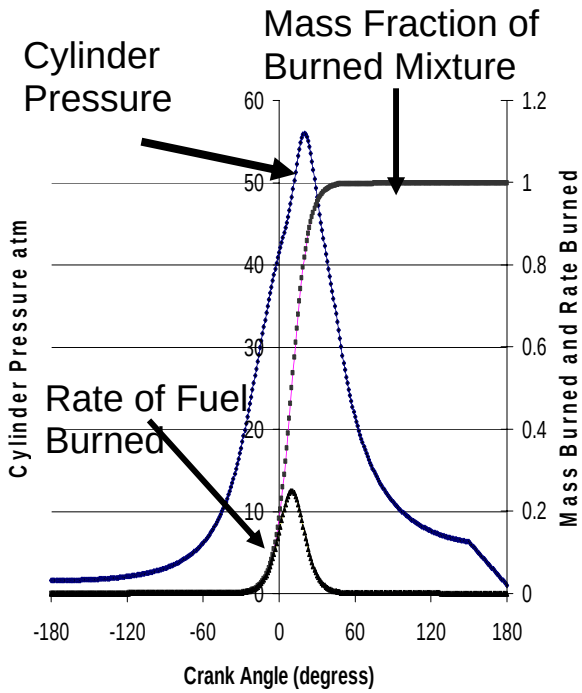


Figure (1) – The distribution of cylinder pressure, mass fraction of burn mixture, and rate of fuel burned. CH4/H2 mixture with and equivalence ratio of 0.6, Engine rpm 2000 and inlet pressure of 1.6 atm.

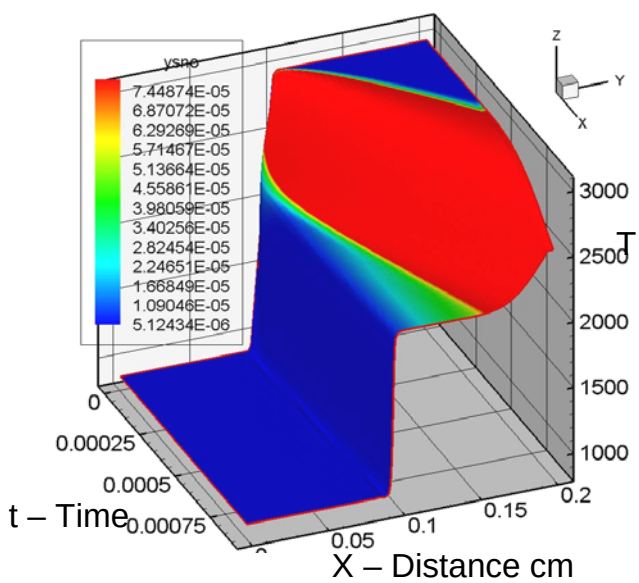


Figure (2) – Time accurate simulation of flame structure. CH4/H2 mixture with and equivalence ratio of 0.6, Engine rpm 2000 and inlet pressure of 1.6 atm.

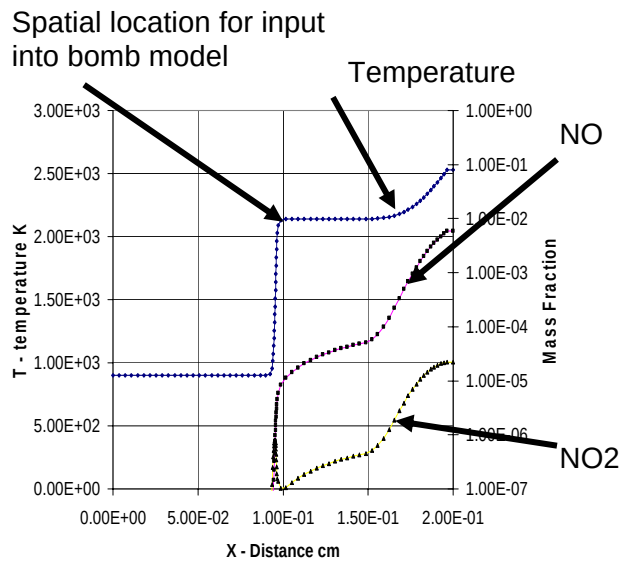


Figure (3) – Distributions of temperature, NO, and NOX in flame simulation at final time. CH4/H2 mixture with and equivalence ratio of 0.6, Engine rpm 2000 and inlet pressure of 1.6 atm.

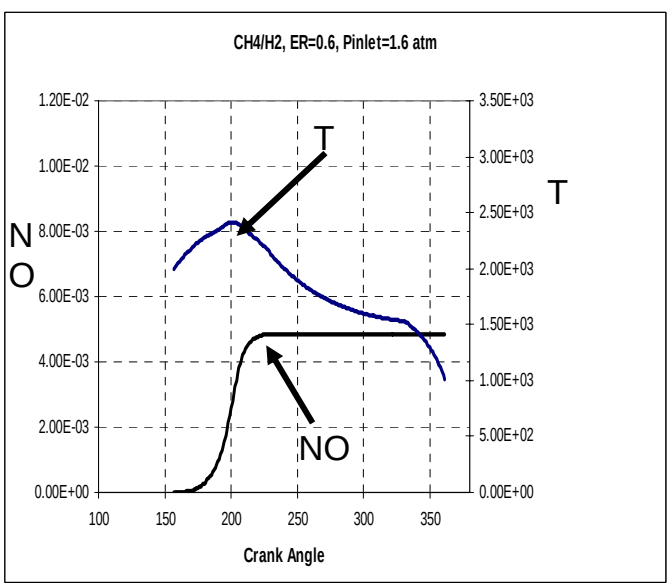


Figure (4) – Variation with crank angle of temperature and NO for fluid parcel close to ignition. CH4/H2 mixture with and equivalence ratio of 0.6, Engine rpm 2000 and inlet pressure of 1.6 atm.

engine cycle. This assumption is partially justified by the expansion of the gases, as well as the higher temperatures, which tends to substantially reduce turbulent mixing.

In order to obtain the time evolution of the fifty three species in the GRI mechanism with the engine pressure variation, we have developed an operator splitting technique to separate the temperature changes due to compression from those due to chemical reactions. The procedure consisted of first solving the flame equations without the spatial terms, and this is equivalent to a homogeneous bomb model. Then the gas mixture was compressed based on the multi-component values of $C_p$ *and* $C_v$ with the species frozen. This procedure was essentially converged for a time step equivalent to one crank angle at 2000 rpm, however we have chosen to use one tenth of a crank angle for all the results presented in this paper.

As is well known the fluid parcels that usually contain the most NOx are those that are formed near ignition, since they are exposed to engine compression for an extended period of time. Shown in Fig. 4 is the time evolution of temperature and NO of these fluid parcels for the lean CH4/H2 engine with 33% hydrogen by volume. For these conditions the temperature increases until twenty degrees after TDC, and there is a very rapid rise in NO and NO2 (not shown). However, as the combustion process ends and the cylinder expands the temperature of the fluid parcel decreases rapidly, and the NO products chemical freeze at a high value. For the lean conditions this fluid parcel is not typical to later crank angles where a much larger portion of the fuel burns at much lower values of NO.

For conditions near stoichiometric the formation process of NO is substantial different due to the much higher temperatures of the combustion products in the engine. Typical results are shown for a stoichimetric mixture of CH4 and air, and it is clear that there is a large overshoot in NO in the engine cylinder. This overshoot is caused by the higher temperatures that exist during the expansion process, which allows the NO to relax to lower values before they chemical freeze. It is clearly seen from these results that the amount of NO is a delicate balance between temperature, engine rpm, and the chemical time scale for a reaction.

In order to obtain the amount of NOx at a given condition in a given engine, we have to assemble all the fluid parcels that have been followed, and we have to weight those fluid parcels with a weighting function which accounts for the amount of fuel burned at the crank angle where the fluid parcel was initially formed. The weighting function is the rate of fuel burned multiplied by a time step associated with the condition of burning. In our simulations we have created fluid parcels every 5 degrees of crank angle, and the rpm was 2000. In general we feel that the present model captures the essence of NOx production in a CNG/H2 engine, and we believe that it predicts a useful value for a given engine. The predicted value of NO does neglect the effects of the mixing of engine products, and it also neglects the effects of fluid stretch caused by engine turbulence. We will discuss these influences after we present the results in the next section of the paper.

RESULTS – We will begin the results section for an engine running on pure CH4 at an equivalence ratio of one, since this result is probably more familiar to most readers of the paper. Shown in Figs. 6 and 7 are the time evolution of NO and temperature, respectively, for selected fluid parcels during the burning of the fuel. The fluid parcels that burn at -25, 0, +10, +20, and +30 degrees with respect to TDC give a good representation of NO formation and they are shown in the figure. At a crank angle of -25 there is the most NO formed, however fluid parcels near this location at not very important, since most of the fuel is burned at later crank angles. The major contribution comes from crank angles between +10 and +20, and the curves in figure 6 decrease with an increase in crank angle. Although there are significant differences in NO values during the engine cycle, the final values of NO are quite similar for combustion at all crank angles. The reason for this behavior can be seen from the temperature curves presented in Fig. 7. It appears that the chemical freezing of NO occurs in a temperature range between 2200 and 2300 for the pressures and rpm of this engine. As should be expected, the weighted value or average value of NO in the exhaust under these conditions is high, and this value for the mass fraction of NO is $2.74x10^{-3}$. In general, for all the results in this paper the values of NO2 have been 15 times smaller than NO, and therefore have not been reported in detail.

The qualitative behavior of NO production under lean conditions is much different, and results are shown in Figs. 8 and 9 for a CH4/H2 mixture with an equivalence ratio of 0.6. Due to lower temperatures NO chemically freezes at much earlier crank angles. Only near ignition does the temperature of the fluid parcels become higher than 2300 K, and again these early burning fluid parcels are not very important since very little fuel burns. The important fluid parcels only have a short time at temperatures above 2200 K, and there is not enough time or intensity to create significant NO or NOx. The overall average of NO mass fraction is $4.30x10^{-4}$, and this a very low value.

Due to the exponential sensitivity of most chemical reactions to temperature, it is not surprising that we should observe some unusual sensitivities of our results to mixture stoichiometry. One of these sensitivities has been discovered for a lean mixture of CH4/H2 (33% H2) at an equivalence ratio of 0.7. Linear thinking would lead one to believe that there would be significantly less NO compared to a mixture of pure CH4 at an equivalence ratio of 1.0. However, the results of our simulations give a rather surprising result, which is shown in Figs. 10 and 11. At an equivalence ratio of 0.7 the temperature of the flame products are significantly lower than the stoichiometric condition, however they are significantly higher than the 2200 K chemical freezing temperature of NO that we observed previously. Therefore, the NO values in Fig. 10 freeze at a much higher value than those for an equivalence ratio of 0.6. The values of NO near the start of ignition are much higher than even the stoichiometric condition, and this is directly due to chemically freezing the NO at the right part of the engine cycle. Just as the engine NO reaches large values at later crank angles, the NO freezes as the temperature of the parcel goes below a critical value.

The NO values in Fig. 10 all chemically freeze at significant values, and the overall average value of the NO mass fraction is $2.80x10^{-3}$ and this is almost the same value as the stoichimetric condition presented previously. An inspection of the temperature histories for the fluid parcels again shows that the NO is produced for temperatures above 2200 K, and it quickly freezes when the temperature goes below 2200 K. For lean mixtures the NO is produced relatively late in the engine cycle, and if NO is produced near the chemically freezing point, there is a significant chance of large values of NO forming in the engine exhaust. It is difficult to make general statements at this time, since typical engines may operate over a wide range of rpm, inlet pressures, and compression ratios for example. However, tools like the present model can be used to define sensitivities, and as computers become more powerful these models can be enhanced and extended.

A summary of the predicted NO values in the engine is given in Table I. It can be seen that similar results for NO are obtained for pure CH4 under lean conditions, and that our results are not sensitive to inlet pressure. However, it we should remind the reader that there are many other considerations for a well working engine, and some of these are the following: (1) Unburned hydrocarbons; (2) Carbon monoxide formation; (3) The ability to burn the fuel under MBT conditions; and (4) Inlet temperature. For most of the other considerations the use of hydrogen in the mixture is a definite advantage. However, hydrogen does of the disadvantage of occupying a large volume.

| **Engine Conditions – all at engine rpm=2000** | **NO Mass Fraction** |
|---|---|
| **Pure CH4,** $\phi = 1.0$, $p_{inlet} = 1.6\ atm$ | $2.74x10^{-3}$ |
| **CH4/H2 (33% H2 by Volume),** $\phi = .6$, $p_{inlet} = 1.6$ | $5.07x10^{-4}$ |
| **CH4/H2 (33% H2 by Volume),** $\phi = .7$, $p_{inlet} = 1.6$ | $2.80x10^{-3}$ |
| **Pure CH4,** $\phi = .6$, | $5.21x10^{-4}$ |

| | |
|---|---|
| $p_{inlet} = 1.6\ atm$ | |
| **Pure CH4,** $\phi = .7$, $p_{inlet} = 1.6\ atm$ | $2.54x10^{-3}$ |
| **CH4/H2 (33% H2 by Volume),** $\phi = .6$, $p_{inlet} = 1.2$ | $4.30x10^{-4}$ |
| **CH4/H2 (33% H2 by Volume),** $\phi = .7$, $p_{inlet} = 1.2$ | $2.50x10^{-3}$ |

**Table I – Summary of exhaust NO in the engine as a function of fuel mixture, equivalence ratio, and inlet pressure.**

Discussion – In the present paper we have used a detailed chemical model to describe NOx formation in an engine. We have not used detailed fluid flow, however we have used the burning characteristics of the fuel to obtain a realistic description of NOx formation with varying pressures and temperatures due to compression and expansion of the gas mixture. We believe that the two major uncertainties in this approach are fluid mixing after combustion, and the influence of turbulent stretch on the details of the combustion process. The influence of turbulent stretch for mixtures of CH4 and H2 could influence the combustion process, since H2 could diffuse preferentially inside the flame into regions of different stoichiometries. This type of behavior has been observed for simplified two-dimensional flows [14], however a complete three-dimensional simulation of CH4/H2 mixtures under engine conditions is presently beyond the scope of current simulations methods. It should also be mentioned that measurement of turbulent flame structure under engine conditions is extremely challenging, and it will be some time before detailed measurements will be made available.

Another reason that NOx is a good candidate to simulate with the present model is that NOx values are a strong function of temperature. Since the temperature of the mixture is mainly a function of stoichiometry and compression ratio, the present model should be expected to yield quite reasonable results. The influence of flame stretch on CH4/H2 mixtures could be partially studied by developing a time-dependent stagnation point flame code, and this being considered by the authors.

## CONCLUSION

The major conclusions of this paper are the following:

1. A new dynamic model for the production of NOx in CNG/H2 fueled engines has been developed and applied to an engine.

2. The model applies the GRI 3.0 chemical kinetic mechanism to the combustion process, and it takes into account detailed local flame structure, and the variation of NOx due to compression and expansion of the products of combustion.

3. The model neglects the influence of mixing of combustion products after combustion, as well as the influence of turbulence on flame structure.

4. Simulations of CH4 and CH4/H2 mixtures has yielded NOx values that are typical seen in the field. This true over a range of equivalence ratios that range from stoichimetric to very lean.

5. The model predicts that lean mixtures of CH4 and H2 can produce very low values of NOx.

6. The results indicated that there is high sensitivity of NOx to equivalence ratio. For example, the variation in NOx between equivalence ratios of 0.7 and 0.6 can vary by almost and order of magnitude.

## REFERENCES


1. K. Bruch, "The Caterpillar 3406 Spark Ignited Low Emission Natural Gas Engine", ASME 91-ICE-5.
2. N.J. Beck, W.P. Johnson, P.W. Peterson, "Optimized EFI for Natural Gas Fueled Engines", SAE 911650.
3. G. Hundleby, J.R. Thomas, "Low Emission Engines for Heavy-Duty natural Gas Powered Urban Vechicles, Development Experiences", SAE 902068.
4. P. Dimplefeld, J. Mack, "Design and Testing of a Natural Gas Fueled Rotary Engine", SAE 920307.
5. K. Collier, R.L. Hoekstra, C. Jones, D. Hahn, "Untreated Exhaust Emissions of a Hydrogen Enriched CNG Production Engine Conversion", SAE 960858.
6. Gregory P. Smith et. Al., "GRI-MECH 3.0", http://www.me.berkeley.edu/gri_mech/
7. H. A. Dwyer, "CHEM_WORK6 - A Personal PC Program for Ideal Gas Equilibrium Calculations with IC Engine Applications", UC Davis, 2002.
8. A. Ochoa, H.A. Dwyer, J. Wallace, "Emissions from Hydrogen Enriched CNG Production Engines", SAE 02FFL-166
9. Heywood, J.B., "Internal Combustion Engine Fundamentals", McGraw-Hill Book Company, New York, 1988.
10. Reynolds, W.C., STANJAN: Version 3.8C, May 1988, Stanford Univ.
11. Kee, R.J., Rupley, F.M., and Miller, J.A. (1990). CHEMKIN II, Sandia National Laboratory Report SAND 89-8009, 1989.
12. MATLAB, Version 6.1, Mathworks Corporation, 2001.
13. H.A. Dwyer, T. Hasgawa, ""Some Flows Associated with Premixed Laminar Flame Propagation in a Rotating Tube Flow", Proc. Of the Comb. Inst., Vol. 29, 2002.
14. H.G. IM, J.H. Chen, "Preferential Diffusion Effects on the Burning Rate of Interacting Turbulent Premixed Hydrogen-Air Flames", Combustion and Flame 131:246-258 (2002).


## CONTACT

For further information about this paper please contact Professor Harry A. Dwyer at the University of California at Davis. The e-mail address is hadwye@ucdavis.edu.

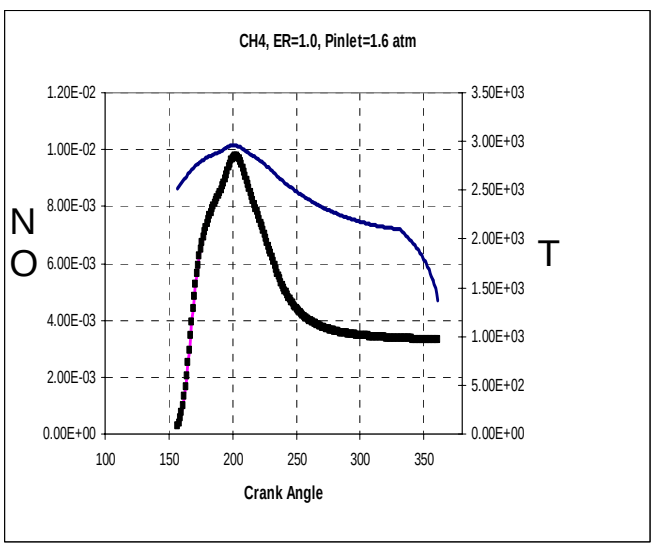


Figure (5) – Variation with crank angle of temperature and NO for fluid parcel close to ignition. Pure CH4 with and equivalence ratio of 1.0, Engine rpm 2000 and inlet pressure of 1.6 atm.

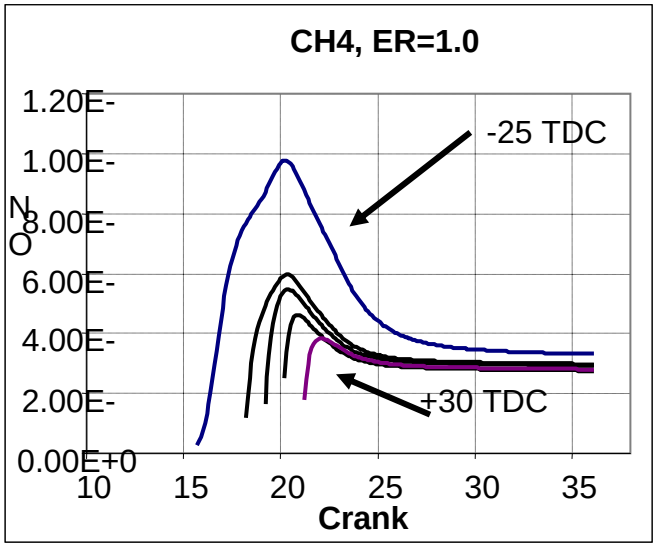


Figure (6) – Variation with crank angle of NO for a distribution of fluid parcels during engine combustion. Pure CH4 with and equivalence ratio of 1.0, Engine rpm 2000 and inlet pressure of 1.6 atm.

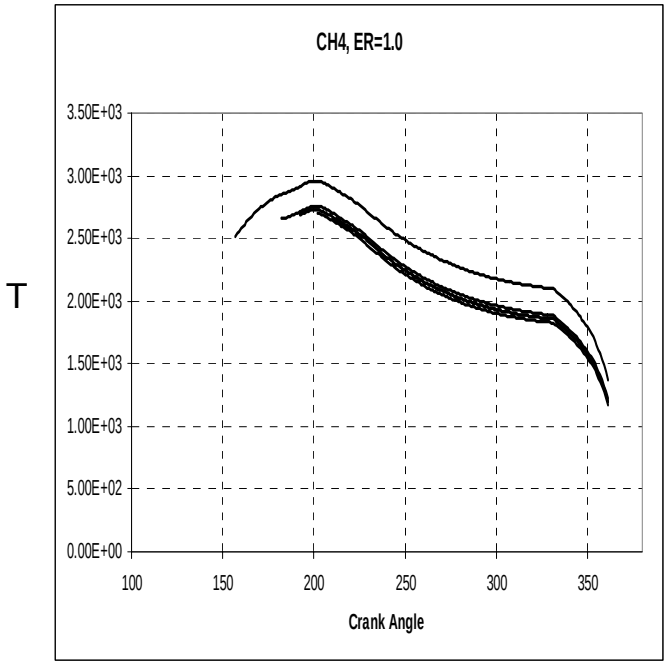


Figure (7) – Variation with crank angle of Temperature (T) for a distribution of fluid parcels during engine combustion. Pure CH4 with and equivalence ratio of 1.0, Engine rpm 2000 and inlet pressure of 1.6 atm.

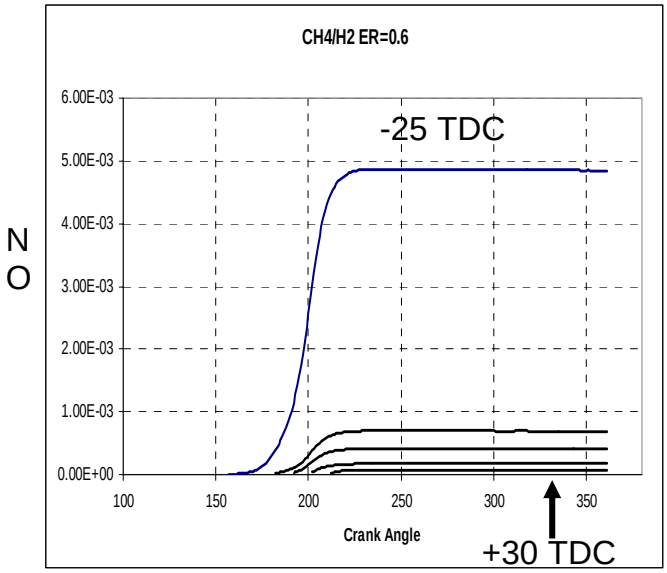


Figure (8) - Variation with crank angle of NO for a distribution of fluid parcels during engine combustion. CH4/H2 mixture with and equivalence ratio of 0.6, Engine rpm 2000 and inlet pressure of 1.6 atm.

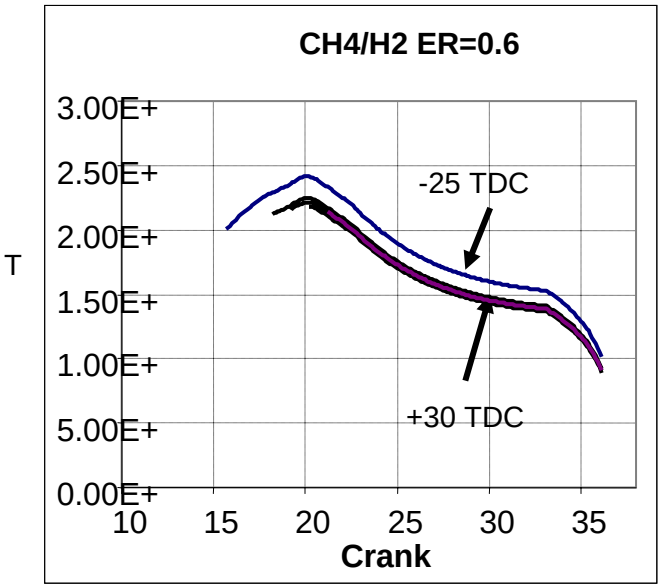


Figure (9) - Variation with crank angle of Temperature (T) for a distribution of fluid parcels during engine combustion. CH4/H2 mixture with and equivalence ratio of 0.6, Engine rpm 2000 and inlet pressure of 1.6 atm.

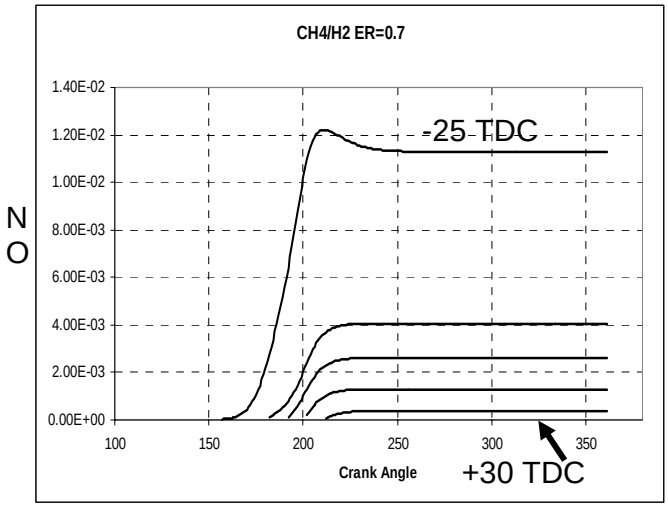


Figure (10) – Variation with crank angle of NO for a distribution of fluid parcels during engine combustion. CH4/H2 mixture with and equivalence ratio of 0.7, Engine rpm 2000 and inlet pressure of 1.6 atm.

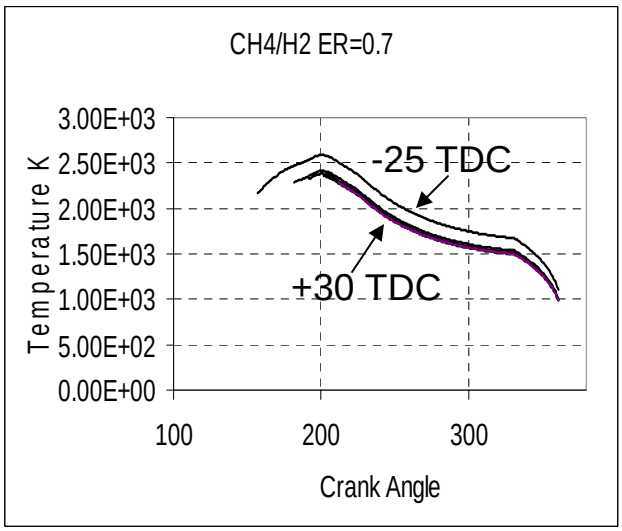


Figure (11) - Figure (8) - Variation with crank angle of NO for a distribution of fluid parcels during engine combustion. CH4/H2 mixture with and equivalence ratio of 0.7, Engine rpm 2000 and inlet pressure of 1.6 atm.